Micropores and micropermeable texture in alkali feldspars: geochemical and geophysical implications

F. David L. Walker, Martin R. Lee and Ian Parsons

Department of Geology and Geophysics, University of Edinburgh, West Mains Road, Edinburgh, EH9 3JW, Scotland

Abstract

Scanning Electron Microscopy and Transmission Electron Microscopy show that normal, slightly turbid alkali feldspars from many plutonic rocks contain high concentrations of micropores, from ~1 μm to a few nm in length, typically 0.1 μm. There may be 10^9 pores mm^{-3} and porosities as high as 4.75 vol.% have been observed, although ~1% is typical. Only 'pristine' feldspars, which are dark coloured when seen in the massive rock, such as in larvikite and some rapakivi granites, are almost devoid of pores. Weathering enlarges prexisting pores and exploits sub-regularly spaced edge dislocations which occur in semicoherent microperthites, but the underlying textures which lead to skeletal grains in soils are inherited from the high temperature protolith. Most pores are devoid of solid inclusions, but a variety of solid particles has been found. Although the presence of fluid in pores cannot usually be demonstrated directly, crushing experiments have shown that Ar and halogens reside in fluids. Some pores are 'negative crystals', often with re-entrants defined by the {110} Adularia habit, while others have curved surfaces often tapering to thin, cusp-shaped apices. The variable shape of pores accounts for the ability of some pores to retain fluid although the texture is elsewhere micropermeable, as shown by ^{18}O exchange experiments.

Apart from rare, primary pores in pristine feldspar, pore development is accompanied by profound recrystallization of the surrounding microtexture, with partial loss of coherency in cryptoperthites. This leads to marked 'deuteric coarsening' forming patch and vein perthite, and replacement of 'tweed' orthoclase by twinned microcline. The Ab- and Or-rich phases in patch perthite are made up of discrete subgrains and the cuspate pores often develop at triple-junctions between them. Coarsened lamellar and vein perthites are composed of microporous subgrain textures. These 'unzipping' reactions result from fluid–feldspar interactions, at T <450°C in hypersolvus syenites and T < 350°C in a subsolvus granites, and are driven by elastic strain-energy in coherent cryptoperthites and in tweed textures. Further textural change may continue to surface temperatures. In salic igneous rocks there is a general connection between turbidity and the type of mafic mineral present; pristine alkali feldspars occur in salic igneous rocks with a preponderance of anhydrous mafic phases.

Because alkali feldspar is so abundant (and larger, 10 μm pores have previously been described in plagioclase), intracrystal porosity is a non-trivial feature of a large volume of the middle and upper crust. The importance of pores in the following fields is discussed: $^{39}Ar/^{40}Ar$ dating and 'thermochronometry'; oxygen exchange; Rb and Sr diffusion; weathering; experimental low-temperature dissolution; development of secondary porosity and diagenetic albitization; leachable sources of metals; nuclear waste isolation; deformation; seismic anisotropy; electrical conductivity. Important questions concern the temperature range of the development of the textures and their stability during burial and transport into the deeper crust.

Keywords: feldspar, alkali, micropores, micropermeable texture.

Introduction

We have investigated the causes of the commonplace turbidity and variable translucency of alkali feldspars and found that they are due to high concentrations of tiny pores (micropores). We describe here the characteristics of the pores and general features of the microtexture that surrounds them. We then

Mineralogical Magazine, September 1995, Vol. 59, pp. 505–534

discuss their formation and assess their considerable geochemical and geophysical implications, developing in more detail, and in the light of subsequent work, implications briefly discussed by Walker (1990). Earlier Transmission Electron Microscope (TEM) work (Worden *et al.*, 1990; Guthrie and Veblen, 1991; Waldron and Parsons, 1992; Waldron *et al.*, 1993) has shown that pores are commonly markers of profound structural and textural changes in feldspars. Their presence in feldspars is a non-trivial feature of crustal rocks, because translucent feldspars are both porous and permeable (Walker, 1990) and the pores are markers of fluid–rock interactions and major rearrangements in the feldspar structure which are almost universal. The pores have important implications for chemical and isotopic exchange in feldspars and for feldspar reactivity with aqueous fluids in the temperature range of diagenesis, soil formation and nuclear waste isolation. They are a significant repository of water and other gases, including noble gases and halogens, in crustal rocks. They may be a factor in the temperature dependence of the rheological properties of the crust, contribute to its electrical conductivity and are one of the factors defining the effective grain dimensions responsible for seismic anisotropy and attenuation.

Previous work

Alkali feldspars are overwhelmingly pale in colour (normally white, grey or pink) and somewhat turbid, causing them to be translucent to chalky in appearance. With very few exceptions alkali feldspars are noticeably more cloudy than quartz in thin section, a feature which is used routinely by petrographers. The translucency is often unevenly developed and cross-cuts clear volumes as veins and patches. In contrast, in some relatively rare rocks, the alkali feldspar is dark green, dark brown or almost black in colour, when seen in the massive rock, and is transparent in small fragments or thin section. The decorative syenite larvikite is the most familiar example of such a rock. Other examples include some dark-coloured rapakivi granites (also a popular dimension-stone) and some charnockites.

Turbidity of alkali feldspars in thin section is usually attributed to 'alteration' which occurred during the cooling of the rock. The cause of this turbidity is at or beyond the limits of optical resolution and is often given no more consideration than a cursory note of its presence. It contributes to the general assessment of rock 'freshness' made by petrographers. It has long been suggested that the turbidity is related to μm-scale features. Folk (1955) suggested that turbidity was not, as was widely believed at the time (e.g. Poldervaart and Gilkey, 1954), the result of 'kaolin-like clay minerals' but was the result of vacuoles, with a much lower refractive index than alkali feldspar, similar to fluid inclusions in quartz. They were more common in acid than in basic rocks. Roedder and Coombs (1967), using light microscopy, reported that perthitic alkali feldspars in granite blocks from Ascension contained up to 10^7 inclusions mm^{-3}. They noted that the inclusions were concentrated in regions of the crystals in which perthite was coarsely exsolved.

Montgomery and Brace (1975), in a Scanning Electron Microscope (SEM) study of plagioclase feldspars, observed pores ranging in size from <1 μm to ~40 μm and measured porosities of up to 2.3% by volume. Higher porosities were found in plagioclase crystals from granitic rocks whose crystallization history had water as an important component, as judged from the presence of primary and secondary hydrous mafic minerals. Plagioclases from the gabbroic, dioritic and metamorphic rocks studied, with relatively dry crystallization histories, had very low microporosities. Montgomery and Brace also suggested that equant pores were the sites of fluid inclusions while planar pores represented healed microcracks. Both types, they suggested, were closely related to the early history of the rock. They did not however (for reasons we discuss below), detect micropores in alkali feldspars. Dengler (1976) also found micropores in plagioclase. These varied in size from <1 μm to 3 μm and were found in greater abundance than in quartz from the same rock.

Parsons (1978) noted that in alkali feldspars from the Klokken layered syenite, the K rich phase of patch perthites was rich in tiny rounded cavities causing them to be turbid, and that the turbidity could be correlated with areas in which regular microperthites were converted to coarse patch perthites. Worden *et al.* (1990) found (by point counting in an SEM) that micropores made up $\leqslant$4.5% by volume of the most turbid Klokken alkali feldspars. Using TEM they also showed that the turbid, coarsely exsolved areas of the crystals were made up of many subgrains (on the scale of a few hundred nm) with the micropores representing gaps between them. The non-turbid feldspar, on the other hand, was devoid of subgrain textures and was composed of lamellar crypto- and micro-perthite. Using TEM, we have since found that, although the details may vary, some sort of major recrystallization of adjacent structure almost always accompanies the formation of pores in alkali feldspar, with the possible exception of uncommon pores formed at high T (Burgess *et al.*, 1992). In the present paper, the presence of a subgrain texture may be taken as implicit in our use of the term 'microporous'. The micropore/subgrain boundary network was shown to render the alkali feldspars micropermeable, in addition to

microporous, by Walker (1990) using ^{18}O exchange and ion microprobe imaging. Parsons *et al.* (1988) showed, using the ^{40}Ar-^{39}Ar step heating method, that natural ^{40}Ar loss from the Klokken feldspars could be correlated with the abundance of micropores. Recently Burgess *et al.* (1992) analyzed the gases extracted from these inclusions by *in vacuo* crushing, using the $^{40}Ar-^{39}Ar$ method, and showed that different generations of inclusion contain fluids with different histories, but do not include a meteoric component. The $\delta^{18}O$ measurements of Parsons *et al.* (1991) confirmed that the Klokken syenites had not interacted significantly with meteoric water. In contrast, Burgess and Parsons (1994) showed, using similar techniques, that very turbid feldspars in the Tertiary Loch Ainort granite from Skye contain a meteoric fluid that had probably interacted with Jurassic envelope rocks.

A number of other workers have inferred that the formation of turbid areas in alkali feldspars is closely related to interaction of fluids with the crystals late in their cooling history at $\leqslant$450°C (Folk, 1955; Montgomery and Brace, 1975; Ferry, 1985; Worden *et al.*, 1990; Guthrie and Veblen, 1991; Waldron and Parsons, 1992; Waldron *et al.*, 1993; Lee *et al.*, 1995). A direct link between turbidity and micropores in feldspars was demonstrated by Ferry (1985). Optically clear alkali feldspars from Tertiary granites from Skye exhibited smooth, featureless surfaces in polished thin section but the surfaces of turbid alkali feldspars showed numerous tiny pits which he suggested were exposed fluid inclusions. Using TEM, Guthrie and Veblen (1991) confirmed that the turbid areas corresponded with areas rich in micropores. Ferry also noted that turbidity corresponded with areas where the alkali feldspar was microperthitic whereas the feldspar was optically homogeneous where clear. The clear areas were subsequently shown by TEM (Guthrie and Veblen, 1991) to be cryptoperthite. Ferry also noted that the $\delta^{18}O$ of the turbid areas was lower ($\delta^{18}O_{SMOW}$ −2 to −6‰) than the non-turbid areas ($\delta^{18}O$ +7 to +8 ‰), suggesting a meteoric origin for the hydrothermal fluids that caused the turbidity, a conclusion confirmed directly by Burgess and Parsons (1994).

Because of their small size there are few reports of direct observation of fluid in pores in alkali feldspars (Roedder, 1984). The multiphase fluid inclusions illustrated by Roedder and Coombs (1967), in feldspars in granitic blocks from Ascension, were exceptionally large (>10 μm) compared with the almost ubiquitous micropores described in the present paper. Feldspars from some pegmatites, including the famous albite from Amelia Courthouse, Virginia, USA, much used in experimental work, contain obvious multiphase inclusions. However, although pores in alkali feldspars from Klokken and Skye are at the limit of optical resolution, the halogens and noble gases extracted by *in vacuo* crushing by Burgess *et al.* (1992) and Burgess and Parsons (1994) show that these otherwise largely permeable feldspars have retained magmatic and meteoric fluids for geological times in some sealed inclusions. Burgess and Parsons have studied a variety of other granitic rocks by the *in vacuo* crushing method and invariably extracted distinctive fluids.

In the present paper we describe the morphology and distribution of micropores, on the scale of tens of nm to several μm, in alkali feldspars from a range of plutonic rock types. Strictly speaking, the smallest possible 'pore' is represented by lattice-scale dislocations, but actual descriptions of dislocations in undeformed alkali feldspars are rare. They were first reported in Or-rich alkali feldspars by Aberdam (1965) who used a carbon replica technique and TEM to study the interfaces of semicoherent microperthite lamellae. Gandais *et al.* (1974) reported periodic dislocations in an Or-rich cryptoperthite and Brown and Willaime (1974) reported dislocations in an Ab-rich ternary mesoperthite. Brown and Parsons (1984) reported semi-periodic dislocations in a strongly ternary mesoperthite and explained how coherency strain and bulk composition control the development of dislocations in alkali feldspars. All these workers used TEM, but Waldron *et al.* (1994) have described a simple HF etching technique which permits dislocations to be displayed using an SEM (e.g. Fig. 7). Lee *et al.* (1995) have shown that subregularly spaced dislocations are common in lamellar Or-rich microperthites from granitic rocks. It is probable that some micropores, particularly in feldspars in weathered rocks, form by simple dissolution of structure around dislocations. However we show below that the majority form during a process in which coherency strain is released by major textural change, and in which the role of dislocations is only secondary.

Methods

In their previous careful studies of micropores in plagioclase feldspars, Sprunt and Brace (1974) and Montgomery and Brace (1975) used ion milling to erode the surface of the crystals. Their intention was to observe surfaces free of pits that might be produced by mechanical polishing; the milled surfaces were expected to have the normal micropore population of the crystal. We compared surfaces produced in three ways: mechanical polishing, atom milling and fresh cleavage fragments produced by mechanical fracturing. These were then imaged with secondary electrons in a Cambridge S250 SEM. The first two methods tended to round off the edges of

TABLE 1. Source rock types, localities, porosities and pore dimensions of alkali feldspars

Sample No.	Rock type	Locality	Age	Colour	Porosity %	±	Length:breadth ratio	Average length μm
DHF-1A	granite	Land's End, England	Carb	white	2.33	0.63	2.19	0.49
DHF-3A	granite	Glen Etive, Scotland	Dev (Caled)	pink	1.57	0.52	2.26	0.43
DHF-4A	granite	Ben Nevis, Scotland	Dev (Caled)	pink	1.13	0.44	2.35	0.56
DHF-5A	pegmatite	Kinlocheil, Scotland	Moine	pink	2.47	0.65	2.14	0.59
DHF-5B	pegmatite (feldspathic)	Kinlocheil, Scotland	Moine	pink	1.07	0.43	2.84	0.42
DHF-5F	gneiss	Kinlocheil, Scotland	Moine	white	2.87	0.70	4.91	0.94
DHF-6A	granite	Loch Ainort, Skye, Scotland	Tertiary	white	0.93	0.40	n/c	n/c
DHF-7B	granite	Beinn Dearg Mhor, Skye, Scotland	Tertiary	green	1.93	0.57	3.34	0.55
DHF-12A	granite	Loch Cluanie, Scotland	Sil/Dev (Caled)	pink	1.33	0.48	2.67	0.63
DHF-14A	tonalite	Torphins, Scotland	Sil/Dev (Caled)	white	1.47	0.50	2.93	0.57
DHF-15A	granodiorite	Correnie, Scotland	Sil/Dev (Caled)	pink/white	1.07	0.43	2.85	0.55
DHF-15C	granite	Correnie, Scotland	Sil/Dev (Caled)	pink	0.80	0.37	2.91	0.52
DHF-16A	granite	Gask, Scotland	Sil/Dev (Caled)	pink	1.07	0.43	2.35	0.33
DHF-16B	tonalite	Gask, Scotland	Sil/Dev (Caled)	white	1.00	0.43	2.13	0.38
DHF-17A	granite	Hill of Fare, Scotland	Sil/Dev (Caled)	pink	1.53	0.51	2.01	0.55
DHF-19A	granite	Ballater, Scotland	Sil/Dev (Caled)	pink	1.47	0.50	2.20	0.34
DHF-22A	granite	Whinnyfold, Scotland	Sil/Dev (Caled)	dark red	1.87	0.57	2.16	0.28
DHF-26A	granite	Nairn, Scotland	Sil/Dev (Caled)	pink	0.67	0.34	2.51	0.47
DHF-27A	pegmatite	Perth, Canada		pink	0.87	0.39	2.70	0.51
DHF-32A	granite	Bodmin, England	Carb	white	1.47	0.50	2.46	0.46
DHF-33A	granite	Shap, England	Dev (Caled)	pink	1.03	0.42	2.29	0.53
DHF-36A	pegmatite	Langesund fjord, Norway	Permian	pink	0.67	0.34	n/c	n/c
DHF-42A	rapakivi granite	Wiborg, Finland	Proterozoic	black	0.40	0.26	n/c	n/c
BM-x	perthosite	Blå Måne Sø. Greenland	Proterozoic	white	2.51	0.64	n/c	n/c
R1-11A	rapakivi granite	Prins Christiansund, Greenland	Proterozoic	black	0.40	0.23	n/c	n/c
43738	laminated syenite	Klokken, Greenland	Proterozoic	white	4.60	0.44	n/c	n/c
140115	granular syenite	Klokken, Greenland	Proterozoic	brown	0.80	0.37	n/c	n/c

n/c = not collected

pores and atom milling led to the obliteration of smaller micropores when compared with fresh cleavage fragments. This may explain the failure of Montgomery and Brace (1975) to report the rather small micropores we found to be almost universal in alkali feldspars. Freshly produced cleavage fragments (as used by Dengler, 1976; Walker, 1990; Worden *et al.*, 1990) preserved the smaller micropores as well as the details of the original shape of the micropores. The majority of pores in the present study were therefore imaged on the (001) or (010) cleavage surfaces using secondary electrons. This approach is open to the criticism that crystals may cleave where micropore concentrations are high. However, back-scattered electron (BSE) imaging of random polished surfaces suggests that this is not the case. Point counting in the SEM was used to determine the microporosity of the samples, on freshly produced, untreated cleavage surfaces. In each case 1500 points were counted over an area of $\sim$46,000 μm^2. Errors were calculated using non-parametric statistical methods as outlined in Conover (1980, p. 100). Longest dimensions and length to breadth ratios were also measured. Because it was impractical to measure porosity at very high magnification, pores smaller than a few tens of nm will have been omitted from the estimates of porosity (Fig. 4). Pores are not evenly distributed in many samples (e.g. Fig. 5) and the values given are for representative microporous areas. We were not able to devise a reliable quantitative method for estimating overall microporosity of a large sample at the scale of a thin section.

The BSE images, obtained using polished sections, were used to determine the distribution of micropores in relation to other intra-feldspar textures (such as any perthitic intergrowths), but this technique is unsuitable for obtaining details of pore size and shape (see e.g. Worden *et al.*, 1990, Figs. 2–4). An excellent way of imaging pores and relating them to the underlying microstructure is gently to etch cleavage surfaces in HF (Waldron *et al.*, 1994) but this modifies and enlarges pores slightly. An example is given as Fig. 7. The method is extremely effective for making the smallest pores visible, and also enlarges and makes visible dislocations, on which etch-pits form rapidly. Micropores are sometimes encountered using TEM and we show examples below and refer to TEM micrographs illustrating pores published by our group and other workers. Care must be taken in interpreting holes in TEM foils as micropores because they may be artefacts of the atom milling or ion thinning of the sample, and can be produced by beam damage in the microscope. However genuine pores commonly have crystallographically controlled outlines, often with discernible outgrowths of new feldspar, crystal inclusions, or an obvious relationship to the surrounding microtexture (e.g. Worden *et al.*, 1990, Fig. 7 and present Fig. 6). In some cases pores seem to have been directly connected with the modification of exsolution microtexture (Waldron and Parsons, 1992, Fig. 8D) or domain microtexture (Waldron *et al.*, 1993). Holes produced during thinning or by beam damage are usually rounded and have edges which diffract weakly in the microscope. Non-feldspar particles in micropores were analysed semiquantitatively using a Link energy-dispersive analysis system on a Cambridge 360 SEM in the Department of Geology and Applied Geology, Glasgow University.

Description of micropores in alkali feldspars

The form and distribution of micropores in alkali feldspars in a wide range of rock types from many localities were looked at in the present study (Table 1). General features are described first, and then we describe the relationship between pores and other features of the feldspar microtexture in examples of hypersolvus and subsolvus syenites and granites.

Shape, size and abundance

Micropores on scales of $\leqslant 1$ μm were irregularly exposed on the cleavage surfaces of all alkali feldspar crystals investigated using secondary-electron imaging, although they were rare in crystals which appeared the least turbid in thin section. In some feldspars micropores were widespread, whereas in others they occurred aligned in rows or in broad strips, corresponding with the irregular bands of turbidity which can commonly be seen in feldspars in section and hand specimen. A representative selection of micropores is illustrated in Fig. 1.

Cleavage surfaces in optically pristine crystals were almost perfectly smooth and were devoid of micropores. Figure 1A shows a cleavage surface of a microperthitic microcline crystal from a 1.7 Ga rapakivi granite from Prins Christian Sund, South Greenland. Three small micropores are visible, but the surfaces are otherwise featureless. Feldspars in this exceptional rock had virtually no pores on any cleavage surfaces inspected and overall had the lowest microporosity (0.4%) found in our study. It is almost black in hand specimen. Comparable feldspars are the glass-clear cryptoperthites from the upper granular layers in the Klokken syenite (Brown *et al.* 1983), which are dark green when unaffected by superficial iron staining, and the nearly black Oslo larvikite, used as a dimension-stone because of its iridescent cryptoperthite.

The remaining micrographs in Fig. 1 are of feldspars which in hand specimen are pale in colour

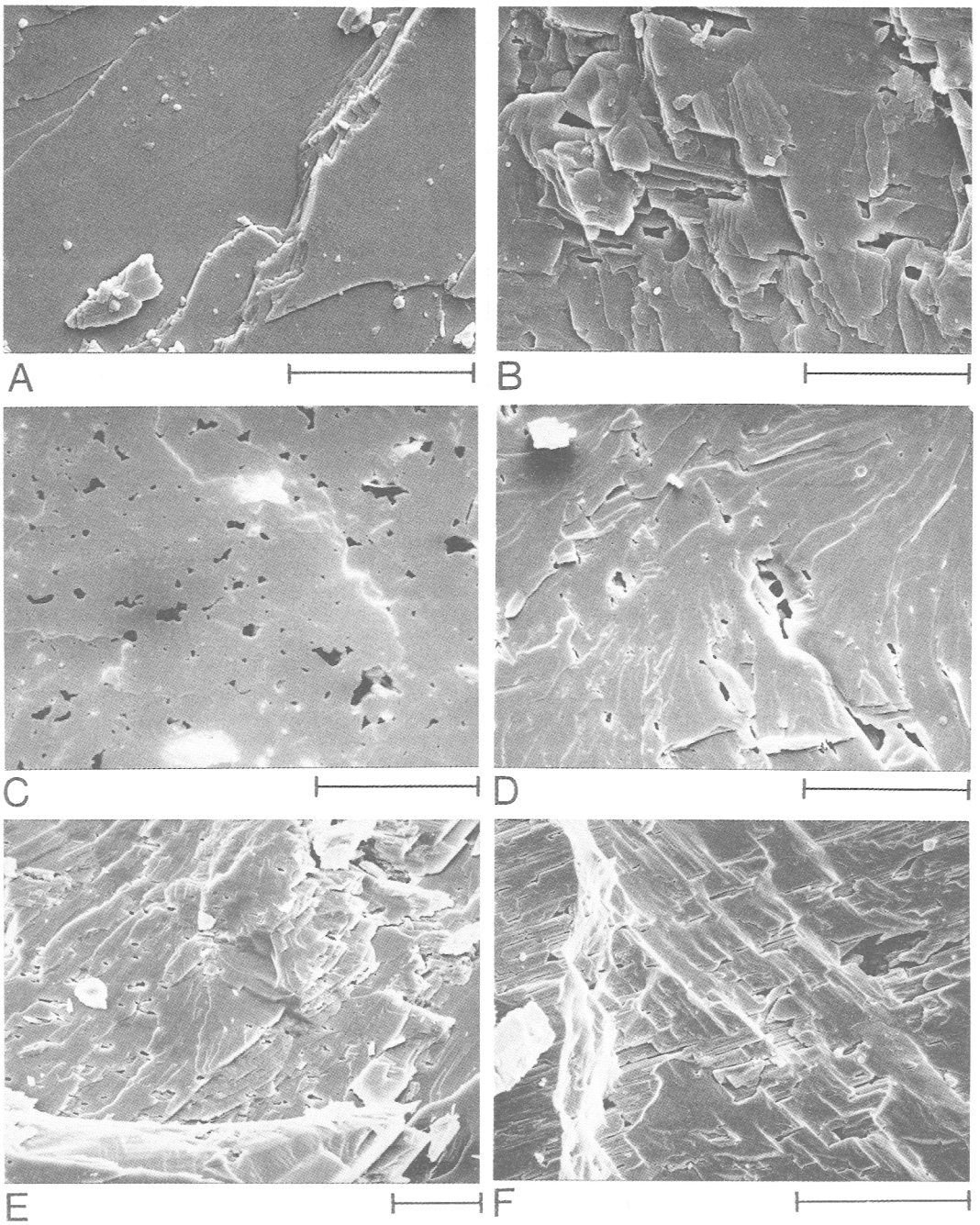

FIG. 1. Secondary electron SEM images of cleavage surfaces of alkali feldspars showing various concentrations and types of micropore. All scale bars 10 μm. (A) Cryptoperthitic microcline from black rapakivi granite, R1-11A, from Prins Christian Sund, South Greenland. The cleavage surfaces are almost devoid of micropores, with three small pores visible to the left of centre. This sample had the lowest microporosity (0.4%) found in the present study. (B) Patch microperthite crystal from laminated syenite, GGU 43738, from the Klokken intrusion, South Greenland. Pores, seen here on (010), are large and angular. In places the porosity of these feldspars reaches 4.75%, the highest recorded in the present study. (C) Patch microperthite from perthosite, BM-x, Blå Måne Sø intrusion, South

and variably translucent. In all cases micropores are readily found as pits on the cleavage surfaces. They commonly display an angular outline (Fig. 1B), forming inverse crystals, but may also have curved outlines, both convex outwards towards the solid, and also inwards towards the void (Fig. 1C). Many pores have a combination of crystallographically controlled and curving surfaces, and populations of pores in individual samples are usually mixed (Fig. 1B,C). Large pores imaged at high magnification (Fig. 2) often have outgrowths on the walls with the characteristic {110} habit of Adularia, and the shape of many pores on the (001) cleavage is defined by the intersection of {010} and {110} planes The growth of new feldspar with the {110} Adularia habit within pores was shown using TEM, by Worden *et al.* (1990, Fig. 7C), and Waldron *et al.* (1993, Fig. 2B,C). This leads to re-entrant angles with the characteristic angle $(110)\wedge(1\bar{1}0)$ of $\sim 59°$ when viewed down [001]. In some cases the pore outlines are defined by planes in the [001] zone, which intersect with (001) at $\sim 116°$ on the (010) cleavage surface. Some pores are connected by narrow zig-zag channels which may represent necking-down of larger pores by the overgrowths (Worden *et al.*, 1990). By changing focus it can also be seen that many micropores 'bell out' below the surface of the crystal, confirming that the micropores are natural features in the crystal and not pluck marks caused by cleaving. This is also confirmed by complex overgrowths within pores (Fig. 2). Common micropore shapes are summarized in Fig. 3.

Figure 4 summarizes the dimensions of pores and the porosities found by point counting. The micropores are normally elongate and typically are around 0.5 μm in length. The majority of micropores in alkali feldspars are thus much smaller than those in plagioclases illustrated by Sprunt and Brace (1974) and Montgomery and Brace (1975), many of which were >10 μm in longest dimension, although the latter authors also found micropores of less than 1 μm. The attention paid by these authors to the larger pores is probably because of the ion-milling method of sample preparation (as discussed earlier). Dengler (1976), who did not use the ion-mill, found pores varying from <1 to 3 μm.

Micropores are ubiquitous in alkali feldspars, confirming earlier suspicions (Parsons, 1978; Parsons *et al.*, 1988) that micropores are common and the main cause of their variable colour and translucency. Almost all of the feldspars studied here came from rocks which, by the conventions of normal petrographic description, would be described as 'fresh'. Microporosity values (Fig. 4) range from 0.4% in black, optically pristine feldspars, to 4.75% in turbid feldspars. The latter value, in a feldspar from a syenite (Fig. 1B) is exceptional, but nevertheless the rock would not, by most petrologists, be described as 'altered', parts of crystals are relatively devoid of pores, and the overall appearance is a silvery-white colour. Figure 1C shows a pervasively turbid feldspar from a perthosite; the overall porosity is 2.5% and the white, chalky-looking feldspar would probably be considered somewhat altered by most petrologists. Ordinary pink or white alkali feldspars from typical 'fresh' calc-alkaline granites, (Fig. 1D,E) have an intragranular microporosity averaging around 1.5%, a significant proportion of the crystal. Figure 1F shows strikingly flattened pores in a feldspar from a felsic band in a gneiss. Pores possibly provide a sub-optical fabric in such rocks, but we have not investigated this in detail.

Weathered surfaces

Weathered surfaces display micropores which are markedly different from those in fresh feldspar. We looked at a series of feldspars from the weathered surface of hand specimens into the interior, and Lee and Parsons (in press) have described in detail the weathering of feldspar phenocrysts from the Shap granite, as well as characterizing the porous microtexture in freshly quarried samples (Lee *et al.*, 1995). Sequential SEM images from normally turbid to weathered feldspars showed a gradation from samples with normal micropore development to samples with immensely enlarged 'etch-pits' and ultimately to complex skeletal shapes. In more markedly weathered areas of the weathered samples we found feathery clay or new feldspar overgrowths; Tazaki and Fyfe (1987) provided SEM micrographs of deeply pitted surfaces of naturally weathered

---

Greenland, imaged on (001). Pores are abundant and somewhat rounded, although some show the intersection of {110} with (001). The overall porosity is 2.6%. These feldspars have a chalky appearance and would be considered somewhat altered by most petrologists. (D) (010) cleavage surface of a striking red potassium feldspar, from the Peterhead granite, DHF-22A, Whinnyfold, Grampian. Pores are aligned parallel to (001). A large pore near the centre has several bridges. (E) (010) cleavage surface of grey alkali feldspar, from the mineralized Cheeswring granite, DHF-32A, Bodmin, Cornwall. There is a high concentration of relatively small pores. (F) (010) cleavage surface of an alkali feldspar from a felsic band in a Moine gneiss, DHF-5F, Kinlocheil, Inverness-shire. In this deformed rock pores are abundant but are strongly flattened and aligned parallel to (001).

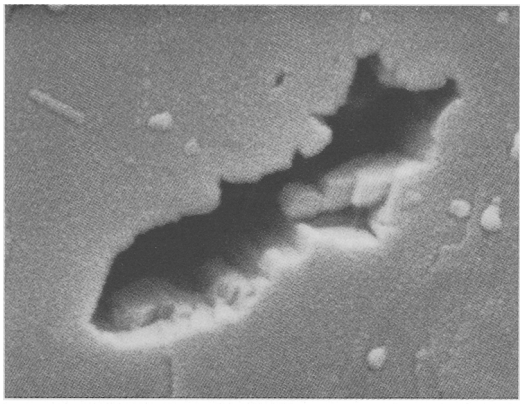

FIG. 2. Secondary electron SEM image of a large micropore in a granular syenite from the Klokken intrusion. Scale bar 1 μm. The main surface is (001). Note the complex shape, with many re-entrant angles, and the prismatic overgrowths within the pore with the {110} Adularia habit. Note also the small pore near the top of the micrograph.

feldspars covered by secondary phases. There is a considerable literature on feldspars in soils illustrating the formation of such etch-pits (Tchoubar, 1965; Lundström, 1974; Wilson, 1975; Berner and Holdren, 1977, 1979; Keller, 1978; Nixon, 1979; Holdren and Berner, 1979; Eggleton and Buseck, 1980; Helgeson *et al.*, 1984; Lasaga and Blum, 1986; Velbel, 1986; Tazaki and Fyfe, 1987; Lee and Parsons, in press). Many workers have implicitly or explicitly assumed that pores (variously called vacuoles, micropores, holes and etch-pits) are always the products of weathering. Helgeson *et al.* (1984) and Lasaga and Blum (1986) provided a theoretical treatment of the development of etch-pits on the basis of 'nucleation' on dislocations. Regularly distributed etch pits of this type have been described by Wilson (1975), and Lee and Parsons (in press) have shown that, in feldspars from Shap, rapid dissolution of elastically strained regions around dislocations on semicoherent microperthite lamellae (Fig. 7) is an important control of weathering rate. It is probable, however, that in many cases it is pre-existing μm-scale micropores that have been enhanced to produce etch pits, because micropores

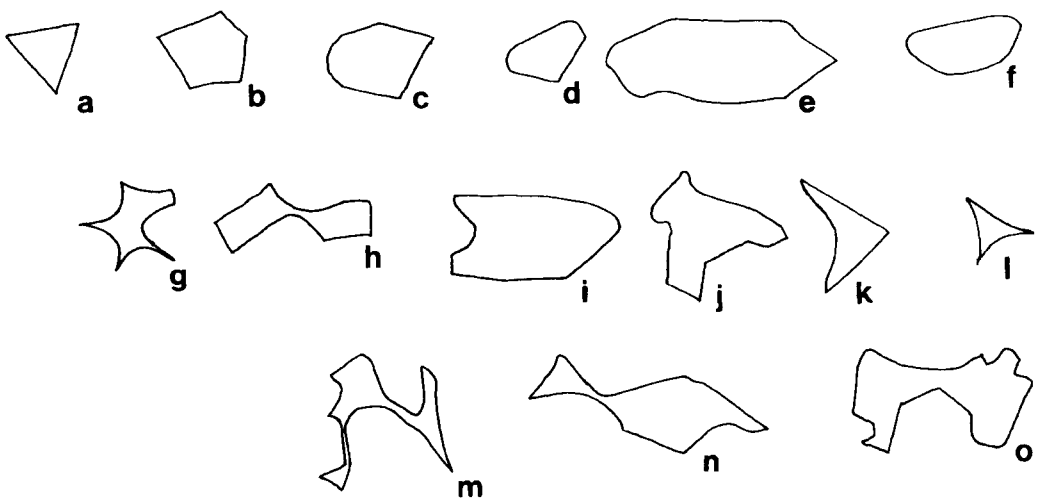

FIG. 3. Common micropore shapes. Although wholly angular equant pores do occur (a), they are rare. More usually some of the edges or corners are rounded and the pores tend to be more elongate (b–e). Wholly rounded micropores (f) are rare also. Most micropores display evidence of feldspar overgrowth resulting in necking down of a single larger pore (h) or simply small rounded (i) or angular (j) outgrowths (see also Fig. 2) from the pore wall. The most common pore form encountered on (001) is (k), with two angular sides representing the intersection of {110} with (001) and with a rounded outgrowth forming the third side (see also bottom right of Fig. 1C). Triangular pores often represent spaces between subgrains (see Fig. 6 and Worden *et al.*, 1990). It is easy to imagine how (l) could represent the point of contact for three rounded subgrains. Pore type (g) represents a combination of subgrain edges and overgrowths. The combination of original pore shape with overgrowths can therefore lead to highly complex pore outlines (m–o) although more simple outlines are more common.

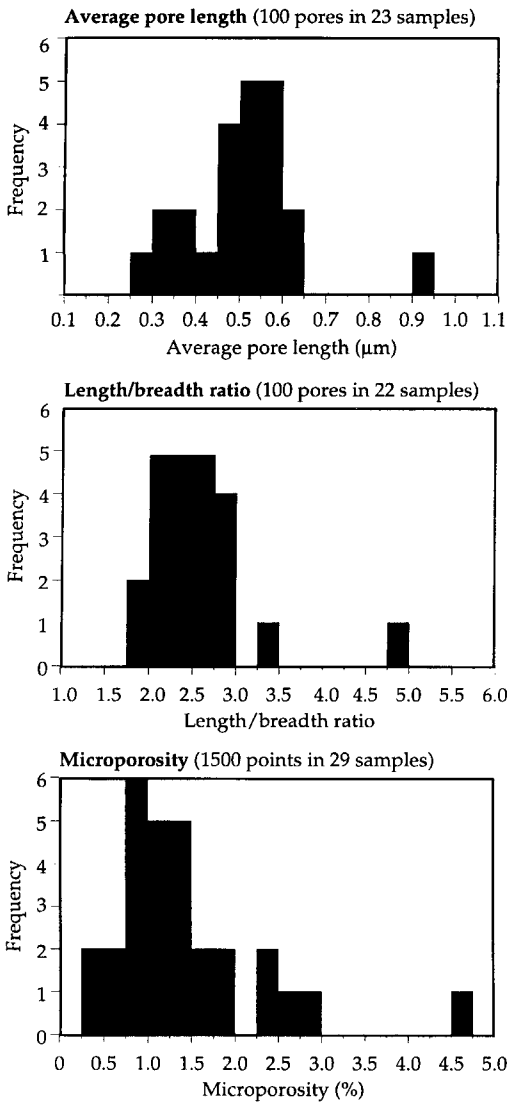

FIG. 4. Histograms of (A) pore length (average of 100 pores in each of 23 samples), (B) length:breadth (100 pores in 22 samples) and (C) porosity (1500 points in 29 samples), for rocks listed in Table 1.

usually lack the periodic distribution characteristic of dislocations in alkali feldspars. During weathering, micropores become more obviously interconnected when compared with micropores from fresh areas, probably because of preferential dissolution along the subgrain boundaries which often link the micropores (see below and Fig. 7).

Alkali feldspars in hypersolvus syenites and granites

Back-scattered electron (BSE) imaging in an SEM (Fig. 5) allows simultaneous observation of micropores and exsolution microtextures, although the resolution is inadequate to distinguish the shape of pores. Parsons (1978) illustrated the correlation between the development of coarse perthites and optical turbidity in alkali feldspars from plutonic rocks. In regular, fine, microperthitic and cryptoperthitic intergrowths, the exsolution lamellae are completely or partly coherent, and the orientation of the lamellae is controlled by the minimization of elastic strain energy (Parsons and Brown, 1984). Depending on bulk composition, they may have a 'braid' or straight lamellar morphology (Brown and Parsons, 1988). Such intergrowths occur in crystals (or parts of crystals) that are largely devoid of turbidity. In contrast, patch and vein perthites, which may be 10^3 times coarser than the strain-controlled intergrowths, are semicoherent to incoherent, have irregular morphologies and almost always correspond with turbid feldspar. These 'deuteric' intergrowths (Parsons and Brown, 1984) commonly occur together with strain-controlled intergrowths within the boundaries of a single crystal.

The BSE method was used by Worden *et al.* (1990) to illustrate the connection between turbidity and coarsening in alkali feldspars from the hypersolvus Klokken syenite; an example is given as Fig. 5A. The bulk composition of the crystals is $\sim(Ab_{60}Or_{40})_{98}An_2$. There is a striking difference between deuteric patch perthites and strain-controlled perthites with respect to micropores, which in BSE show up as black dots on the grey shades of the perthitic feldspar. Micropores are almost completely absent from areas of strain-controlled perthite except for rare isolated pores (Figs. 2, 5A). Curving trails of pores occasionally occur which do not affect the regular exsolution microtexture and which therefore formed at high *T* (see Burgess *et al.*, 1992, Fig. 2a), but other trails clearly affect the microtexture (Fig. 5B) and presumably follow fractures formed at relatively low *T*. Pores are abundant in patch perthites, those in the Ab-rich phase being on average larger but less abundant than those in the Or-rich phase. The change between the two areas is very abrupt (Fig. 5A), with remnants of strain-controlled braid or lamellar perthites occurring completely surrounded by patch or vein perthites. Some crystals may be pervasively affected, or affected only in places in an irregular way (Fig. 5A; see also Worden *et al.*, 1990, Burgess *et al.*, 1992, Fig. 2b, and optical micrograph in Parsons, 1978, Fig. 7). There is sometimes a tendency for pores and coarsening to occur near grain margins, leading to a 'pleated rim' (Fig. 5B). Pleated rims correspond with zones of

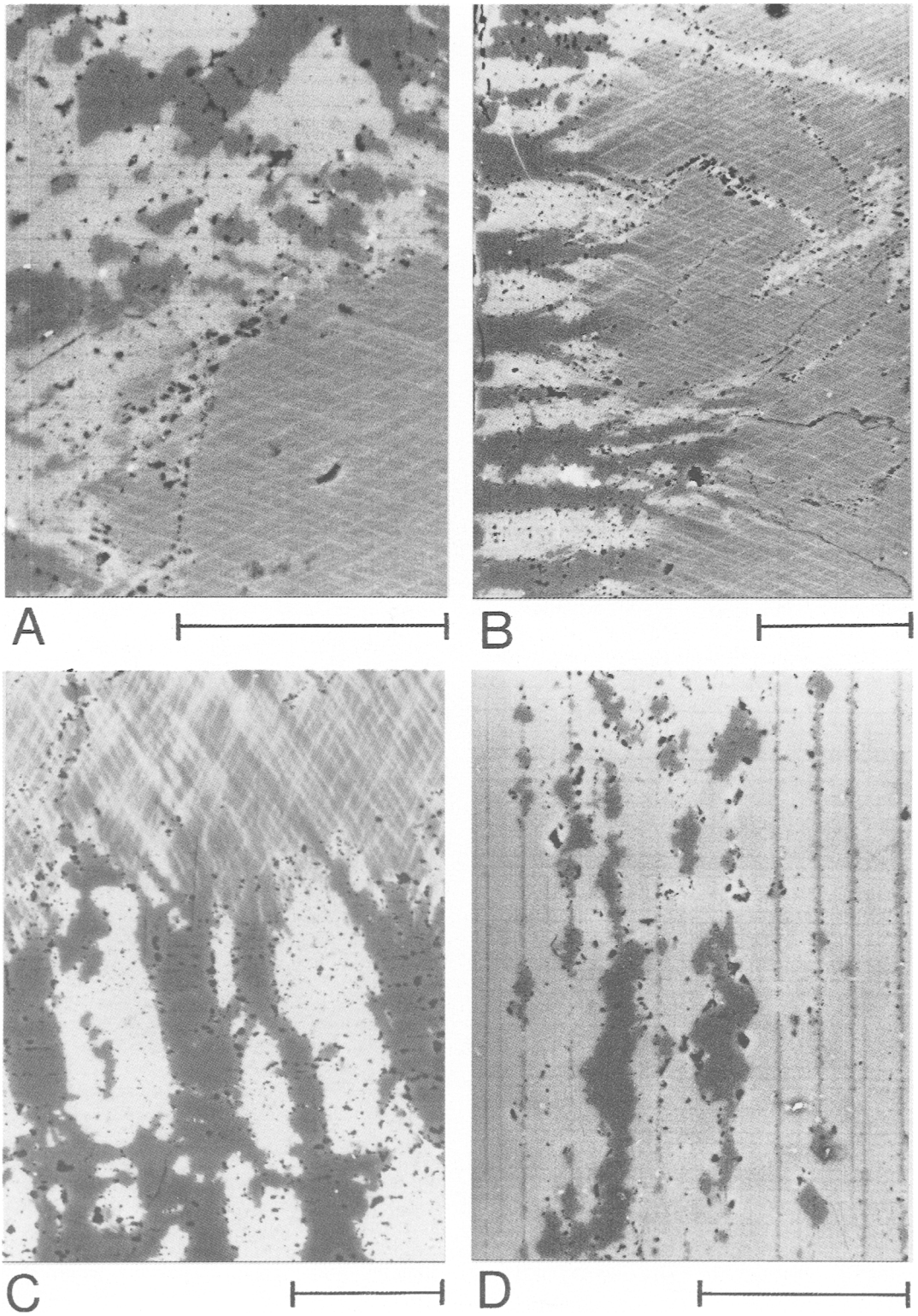
A
B
C
D

turbidity along crystal margins (Fig. 5B; see also Burgess *et al.*, 1992, Fig. 2b, and optical micrograph in Parsons, 1978, Fig. 8b; Lee *et al.*, in prep., treat the development of pleated rims in detail).

Alkali feldspars in hypersolvus granites are often coarse vein microperthites (similar to the lower part of Fig. 5C), which are invariably slightly turbid, and only occasionally contain the pristine, pore-free areas which are common in syenites. Our experience is that feldspars in hypersolvus granites are more pervasively turbid than those in syenites, and that braid perthites are rare in the granites. Lee *et al.* (in prep.) show that the vein perthite develops by encroachment of pleated rims into the interior of the crystals until they meet in the centre. The braid perthite in Fig. 5C is therefore a relic between two advancing sets of pleats. The vein lamellae contain many pores and subgrains and are at least partly incoherent. The resulting texture is considerably more regular than the patch perthite common in syenites (Fig. 5A) but, although coarser, is considerably less regular than the strain-controlled crypto- or micro-perthite in which the pleats initially develop. Some hypersolvus, high-level granites, and, particularly, granophyres have extremely turbid feldspars. The Skye epigranites, in which feldspar textures have been illustrated using BSE and TEM by Guthrie and Veblen (1991), fall into this category. As we discuss below, these different degrees of turbidity probably reflect phases of extended fluid–feldspar reaction which exploit textural features that were acquired in an initial phase of pore formation.

Worden *et al.* (1990) imaged micropores in the turbid parts of Klokken feldspars by TEM. The strain-controlled microtexture is completely recrystallized to a mosaic of subgrains in turbid regions. (Strictly speaking, the term subgrain implies slight misorientation between volumes of structure surrounded by subgrain walls. Measurable misorientation of the *average* structure often does not occur between subgrains in perthites, but the walls persist both because of difference in composition and because of misfit between adjacent ordered–antiordered twins and tweed domains.) There is clearly a direct connection between the development of turbidity, the presence of pores and profound changes in the crystal microtexture. The pores frequently lie at points of connection between networks of subgrain boundaries (Fig. 6A,B). The subgrains themselves often have the Adularia habit and the shape of pores is often defined by outgrowths of new feldspar with the Adularia habit (Fig. 6; also Worden *et al.*, Fig. 7C). Waldron and Parsons (1992) illustrated an example of an isolated pore in a strain-controlled microtexture which appeared to be associated with a trail of recrystallized microtexture. Lee *et al.* (in prep.) have studied the development of pleated rims and vein perthite (Fig. 5B,C) using TEM and these too involve breakdown of strain-controlled microtexture to a mosaic of subgrains and associated pores.

Alkali feldspars in subsolvus granites

Despite the abundance of Or-rich feldspars in subsolvus granites there are few systematic descriptions of their microtextures. Lee *et al.* (1995) described the pink phenocrysts from the granite from Shap, northern England, and we have found the

FIG. 5. Back-scattered electron images of alkali feldspars, using an SEM, showing relationship of pores with exsolution textures. All scale bars 40 μm. Micropores appear black, albite is medium grey and K-feldspar is light grey. All images are viewed approximately parallel to [001]. (A) Boundary between braid cryptoperthite (bottom right) and pervasive patch perthite, laminated syenite, Klokken intrusion. The braid perthite is devoid of pores except for one large pore which does not affect the microtexture and which therefore developed before exsolution. There are many pores in the patch perthite, particularly near the edge of the braid perthite. (B) Pleated rim (Lee *et al.* in prep.) on braid cryptoperthite, Klokken syenite. The pleats have developed inwards from the surface of the crystal which is at the extreme left of the micrograph. Micropores are common in the pleats but in the interior of the crystal occur only as trails and bands crossing the pore-free braid cryptoperthite. The braid texture is modified in these bands, showing that they formed subsequent to exsolution, probably along cracks. (C) Boundary between braid perthite (top) and vein perthite (bottom) in a feldspar from a quartz-syenite aplite cutting the Klokken intrusion. Pores are again restricted to the vein perthite, which forms by propagation of pleated rims throughout the entire crystal. The head of a set of advancing pleats is just visible at the top of the micrograph, together with the associated micropores, and the braid perthite is a relic in a crystal largely made of vein perthite. Many alkali granites contain vein perthite exclusively. (D) Mixed lamellar and patch microperthite in a phenocryst from the Shap granite (Lee *et al.* 1995). The albite lamellae are parallel to $(\bar{6}01)$ and, where non-porous, the broader lamellae are semicoherent with sub-regularly spaced dislocations (not visible in this image but see Fig. 7). Some of the lamellae have developed micropores, and, where these are most intensively developed, the perthite has coarsened, leading to much broader areas of albite. Just below centre these have the Adularia habit. Lines of pores also occur which are not associated with contrast in the BSE image of the perthite. These represent regions from which albite has been removed to contribute to the coarsened patch perthite.

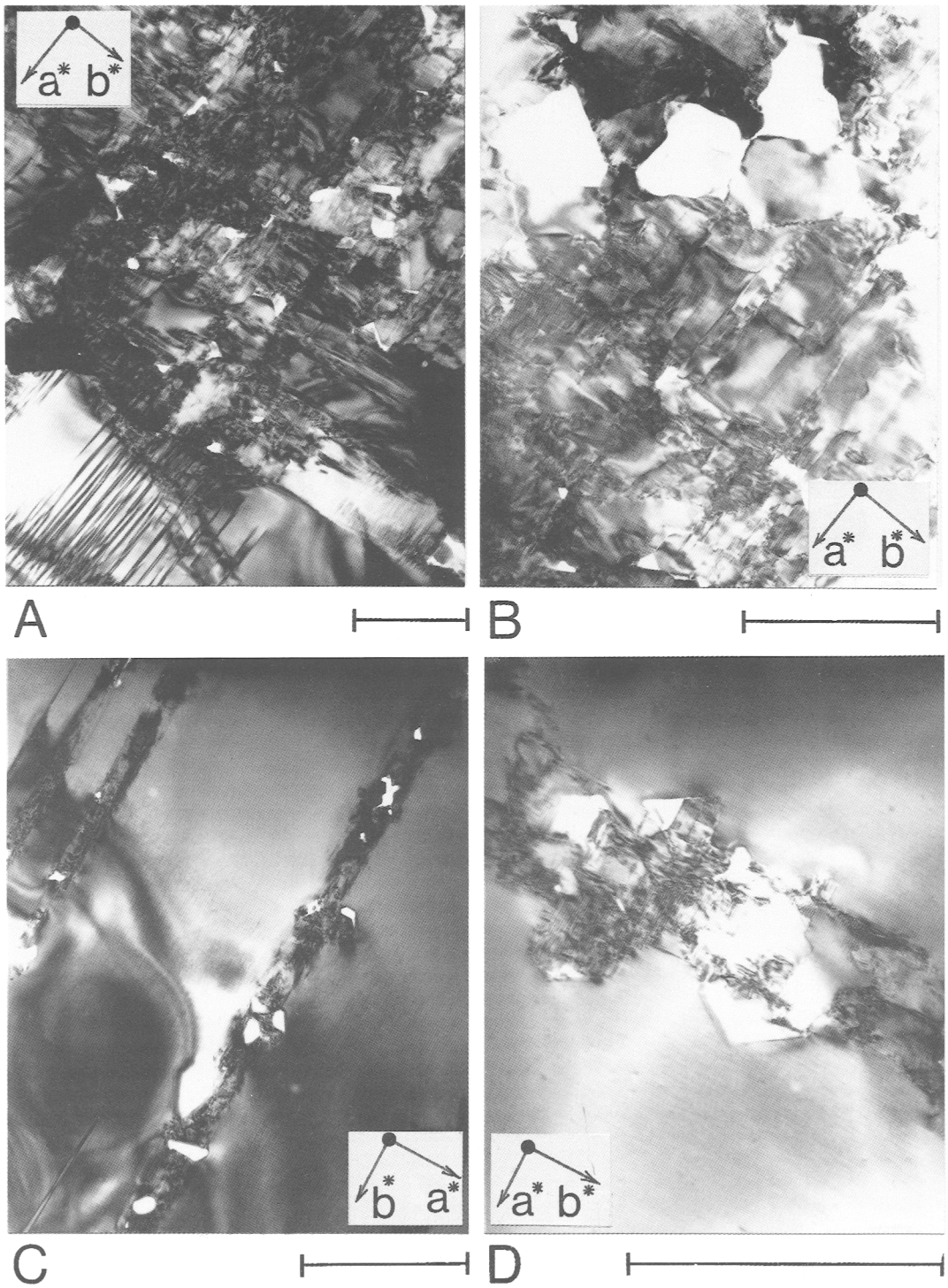

FIG. 6. Bright-field TEM micrographs of microporous alkali feldspars, beam approximately parallel to [001]. All scale bars 1 μm. Micrographs A and B were taken by R.H. Worden. (A) Patch perthite from the Klokken syenite, similar to the top of Fig. 5A. The field is mostly Or-rich feldspar with an area of Albite-twinned albite at the bottom

same general features in alkali feldspars from several Scottish Caledonian granites. Some of the features were illustrated in Waldron *et al.* (1994). Such feldspars are invariably, to some extent, turbid with variable volumes of pristine crypto- and microperthite. Turbidity in such crystals is of two types: irregular bands developed along fractures and cleavages, and turbidity within lamellar, perthitic albite. This second type of development, which is not seen in hypersolvus feldspars with strain-controlled intergrowths, results from a fundamental difference in the original strain-controlled microtexture. Because of their bulk composition (usually close to $Ab_{20}Or_{80}$, with $An_{<1}$), lamellae in pristine orthoclase have the form of flat, oval lenses, in the Murchison plane, $\sim(\bar{6}01)$, extended to form almost straight lamellae on (010) and shorter lenses on (001). The straight, largely coherent, thicker lamellae frequently develop spaced edge dislocations to relieve strain (see Brown and Parsons, 1988, for discussion of the relationship between bulk composition and morphology and type of strain-controlled exsolution texture in alkali feldspars). These dislocations can be readily located by SEM on cleavage surfaces lightly etched in HF and have also been characterized by TEM (Waldron *et al.*, 1994; Lee *et al.*, 1995). Each dislocation forms an extended loop around the lens and thus intersects the cleavage surface twice, giving rise to pairs of etch-pits (Fig. 7). Dislocations occur in two orthogonal directions, and on the lamellar interface $(\bar{6}01)$ they therefore form an orthogonal grid. It is the presence of these dislocations which leads to the preferential development of pores along albite lamellae (Figs. 5D; 6C,D; 7), a phenomenon which does not occur in more Ab-rich perthites with fully coherent intergrowths (Fig. 5A–C). The albite,

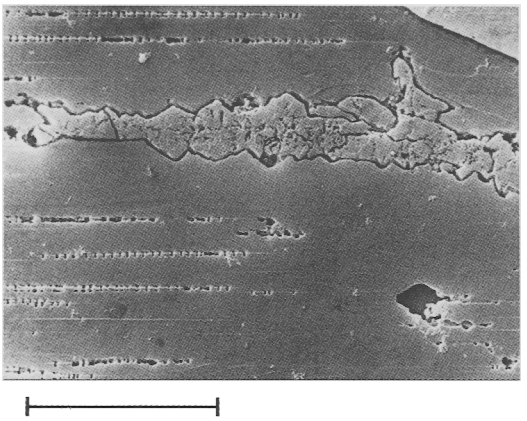

FIG. 7. Secondary-electron image of (001) cleavage surface of a phenocryst from the Shap granite which has been etched in HF vapour (Waldron *et al.*, 1994). Scale bar 10 μm. At the left, fine, fully coherent albite lamellae parallel to $(\bar{6}01)$ are visible because of slight variation in dissolution rate. Thicker lamellae are defined by rows of etch pits representing the outcrop of edge dislocations in $(\bar{6}01)$. The paired dislocations represent the outcrop of extended, lens-shaped dislocation loops. Two thirds up the image a band of deuteric coarsening is composed of subgrains with many micropores. Subgrains frequently show {110} terminations against the enclosing orthoclase.

initially Albite- or Pericline-twinned but continuous, recrystallizes to a subgrain mosaic with outgrowths with the {110} Adularia habit, and pores form between the subgrains (Fig. 7; see also Lee *et al.* 1995). This different behaviour presumably results

---

left. The potassium feldspar is mostly irregularly twinned microcline, with a few areas of tweed orthoclase, featureless at this scale, and it is broken up into numerous subgrains defined by conspicuous walls parallel to {010} and a few walls parallel to {110} (relative to the average monoclinic symmetry). There are 35 pores visible in the micrograph ($\sim 8.5 \times 10^9$ pores mm^{-3}), at a variety of scales up to ~300 nm. Many are defined by {010} and {110}. A pore in the centre of the micrograph (and several others) contains a distinct outgrowth with the Adularia habit. (B) Higher magnification image of a similar area of irregular microcline and tweed orthoclase. Subgrain walls, somewhat curved or wavy, but generally parallel to {110} and {001}, are conspicuous. They are sometimes visible because of minor beam damage, or more commonly by localized strain shadows, and they sometimes die out laterally. A group of relatively large micropores occurs at the top of the micrograph, partly curved in outline, but with a conspicuous {110} surface defining a pore at the left. Pores commonly occur at triple-point junctions between subgrains; a number of small pores at the bottom left show this relationship particularly clearly. (C) Lamellar microperthite in a phenocryst from the Shap granite, similar to Fig. 5D. The bulk of the micrograph is tweed orthoclase. At the bottom left and top left thin albite lamellae are fully coherent and devoid of pores, but thicker lamellae contain numerous pores and are composed of microcline that has replaced albite. Note that such lamellae would be invisible on Fig. 5D, because of the lack of atomic-number contrast, although the trains of pores would be visible. The thicker lamellae were permeable to fluids because of subregular edge dislocations like those shown by etch pits in Fig. 7. (D) Detail of lamella of replacive microcline in tweed orthoclase. Pores, subgrains, and peg-like extensions of microcline into the tweed orthoclase all have the Adularia habit.

TABLE 2. Elements detected in non-feldspar phases in micropores

Sample	Location	Analysis No.	Elements detected
DHF-3A	Cruachan	1	Na, S, Pb
		2	S, Ca, Ba
DHF-6A	Loch Ainort	1	Na, Cl
		2	Na, Cl
DHF-16A	Skene	1	Sn
		2	Cl, Ag
		3	S, Ag
		4	S, Ag
DHF-17A	Hill of Fare	1	Fe
		2	Cl, Fe
		3	Fe
		4	Fe
DHF-19A	Ballater	1	Fe
		2	Ca
DHF-22A	Peterhead	1	Fe
		2	Al, Fe
		3	Al, Fe
DHF-33A	Shap	1	Mg, Ti, Mn, Fe
		2	Mn, Na, Cl, Ti
		3	S, Ca, Ba
43738	Klokken (laminated syenite)	1	Cl, Ti, Fe
		2	Na, Fe
		3	Fe
140025	Klokken (granular syenite)	1	Fe
		2	Fe
		3	Ba Fe

from permeation of water down those dislocation cores which intersect the surface, into the interior of the crystal. The subgrains may be of albite, in which case the local bulk composition remains approximately constant, or may be microcline (Fig. 6C,D), in which case the bulk composition has locally changed and the intergrowth is no longer strictly a perthite. In other parts of the same crystals bands of recrystallization occur, along early fractures. The textures in these bands are similar to those associated with pervasive turbidity and recrystallization in more Ab-rich microperthites. The etching technique is particularly effective at showing the relationship between pores and the underlying subgrain texture, without the extended preparation of TEM work (Fig. 7; see also Waldron *et al.*, 1994).

Other minerals in micropores

Although it is frequently suggested that the colour of feldspars is caused by included particles, particularly of hematite and magnetite, the overwhelming majority of pores inspected by SEM did not contain other minerals. Many contain distinct overgrowths of new feldspar (Worden *et al.*, 1990, Fig. 7C,D). Waldron and Parsons (1992, Fig. 8D) illustrated a pore with a partial infilling of feldspar which appears to be associated with a trail of recrystallized structure. A few pores contain clay minerals (Worden *et al.*, 1990, Fig. 8) and probable iron oxides (Worden *et al.*, Fig. 7D), but in the absence of a technique for oxygen determination it is difficult to identify the Fe-bearing phase exactly. Using ED X-ray analysis in the TEM, Guthrie and Veblen (1991) found halite, Fe (oxides) and sulphides, and compounds with Mn, Cr, Ti, Cu, Zn, Ni and Mg in granites from Skye. We used ED analysis in an SEM to obtain an indication of elements in included phases in pores in feldspars from a number of rocks (Table 2). Although it was not possible to obtain quantitative analyses, it is interesting that the elements detected were distinctive between different intrusions. For example, Ag-bearing phases were found in the Caledonian granite from Skene, but only Fe minerals were found in the neighbouring granite from Hill of Fare. It would be interesting, but time-consuming, to establish what proportion of the trace elements of granitic rocks is in phases in pores, and

whether they provide any indication of the potential for ore formation.

Relationship between turbidity and igneous rock type

Because of the difficulty of measuring the abundance of pores over large areas of crystals in which they are heterogeneously distributed, we were not able to establish whether an exact, quantitative relationship exists between average microporosity of feldspars in a sample, at the hand specimen scale, and other features of the mineralogy of each rock. Nevertheless, there is often clearly a general correlation between the identity of the mafic silicates and the porosity of the feldspars. A very striking example of turbidity varying with rock units on a very intimate scale was described by Parsons (1978) in the interleaved granular and laminated syenite layers in the Klokken layered syenite. In this case the granular syenites are pyroxene-bearing, with trivial amounts of biotite and usually no amphibole; the alkali feldspars are glass-clear, with a strain-controlled microtexture which SEM work shows to be nearly devoid of micropores (Fig. 5). In contrast, interleaved, laminated syenites often have substantial biotite and amphibole and the feldspars are highly turbid, the porosity reaching 4.75%. Burgess *et al.* (1992) showed that the rare pores in feldspars from the granular syenites, which formed at high T, contain a fluid, released by crushing, with high radiogenic $^{40}Ar/Cl$, characteristic of mantle fluids, whereas a fluid with lower $^{40}Ar/Cl$ (perhaps derived from the other fluid by boiling) was released by pores in the pervasively turbid feldspar in the laminated syenites.

Black feldspars in rapakivi granite samples DHF-42A and R1-11A, from Prins Christians Sund, South Greenland, have the lowest porosity found so far (Fig. 1A). The nearly black or dark green granites and quartz monzonites in the South Greenland rapakivi province are striking rocks in thin section with almost completely non-turbid feldspar and a predominantly anhydrous mafic mineral assemblage, including fayalite, ortho- and clino-pyroxene (Harrison *et al.*, 1990). Small amounts of amphibole form fringes on olivine and orthopyroxene, or sometimes form poikilitic plates enclosing orthopyroxene, and biotite forms reaction rims on amphibole and ilmenomagnetite. In contrast, some units of these plutons, cross-cutting areas within them, and granite in the vicinity of metasedimentary xenoliths, have feldspars which are brownish or creamy-white in colour, and are substantially more turbid in thin section. These variants have a wholly hydrous mafic silicate assemblage, largely amphibole with some biotite. The white facies of the rapakivis is therefore similar to ordinary granites, for example from the Scottish Caledonian, which have pink and white feldspars. Hornblende and micas are overwhelmingly the most common mafic phases.

Generally speaking it seems that alkali feldspars show more deuteric alteration in rocks that have crystallized from more hydrous magmas. This confirms that the observations of Montgomery and Brace (1975) on plagioclase feldspars also apply to alkali feldspars. They showed that plagioclase in rocks with a relatively anhydrous cooling history (e.g. gabbros) was generally free of micropores, whereas that in rocks with a hydrous history (e.g. granodiorites and granites), contained micropores. As we discuss below, the presence of turbidity and associated textural changes are markers of low-T (<450°C) fluid–feldspar interactions. Thus, the water content of the magma appears to be reflected in the degree of deuteric alteration despite the considerable temperature interval between the solidus and the onset of deuteric changes. In the face of the pervasive recrystallization in the feldspars in many granitic rocks, it seems worth questioning whether the hydrous, mafic mineral assemblage is wholly, or even partly, magmatic.

Temperature and mechanism of formation

Temperature range

A few pores in feldspars seem to be primary in origin and to have trapped magmatic fluids (Roedder and Coombs, 1967; Burgess *et al.*, 1992). The pores of this type studied by Burgess *et al.* in feldspars from the Klokken intrusion, formed discrete trails which did not affect the strain-controlled exsolution microtexture in the feldspar host, indicating trapping at >850°C. It is generally agreed by all previous workers, however, that the development of pervasive turbidity and the intense development of micropores occurs late in the cooling history of plutons (Folk, 1955; Montgomery and Brace, 1975; Parsons, 1978; Parsons, 1980; Parsons and Brown, 1984; Ferry, 1985; Parsons *et al.*, 1988; Worden *et al.*, 1990; Guthrie and Veblen, 1991; Burgess *et al.*, 1992). The relationship with other microtextures in feldspars allows an upper limit of temperature to be placed on the formation of pores and subgrains (see also Brown and Parsons, 1993). In the Klokken syenite, braid microperthites composed of zig-zag low microcline and low albite are clearly cut by the deuteric textures (Worden *et al.*, 1990). This implies a maximum temperature of formation of <450°C, the upper limit of stability of low microcline (Brown and Parsons, 1989). In the Coldwell intrusion, linear, coherent cryptoperthites which will have exsolved at ~380°C, are cross-cut by deuteric coarsening. In subsolvus

granites the more Or-rich bulk compositions of volumes of coherent cryptoperthite (which we have commonly observed by SEM and TEM, Lee *et al.*, 1995) imply even lower temperature for the upper temperature range of the deuteric reactions, <300°C.

It is more difficult to place lower temperature limits on the reactions. Pairs of feldspars at known down-hole temperature of 250–350°C are in alkali exchange equilibrium in the Salton Sea geothermal field (McDowell, 1986), and Lidiak and Ceci (1991) have described authigenic K-feldspar replacing and pseudomorphing granite K-feldspars at a buried unconformity. Feldspar grows readily in diagenesis (Worden and Rushton, 1992), commonly with the Adularia habit which characterizes new feldspar growth within pores and in recrystallized structure (e.g. Worden *et al.*, 1990, Fig. 7C; Waldron *et al.*, 1993, Fig 2B-D, Fig. 3; Lee *et al.*, 1995, Fig. 7). Under the appropriate conditions, there seems reason to believe that modification of microporous feldspar can continue at surface temperature with the growth of new feldspar.

Textural environment of micropores

In strain-controlled crypto- and micro-perthites, the development of dislocations is a function of bulk composition (Brown and Parsons, 1984). Dislocations have been identified by TEM at the boundaries of straight, strain-controlled, Or-rich microperthites (Fig. 7; see also Waldron *et al.*, 1994, Lee *et al.*, 1995 and the review of earlier observations in Brown and Parsons, 1984) and in Ab-rich mesoperthites (Brown and Parsons, 1984). These dislocations occur in linear rows, have a subregular spacing and occur in pairs (the outcrops of loops) when observed parallel to the dislocation. Micropores are not, in general, distributed in rows and they are abundant in bulk compositions in which strain-controlled intergrowths are entirely dislocation free (Brown and Parsons, 1984; Worden *et al.*, 1990). Thus micropores do not nucleate directly on dislocations. Only in cases where general recrystallization has been facilitated by dislocations is there any connection between dislocations and pores (Fig. 7). The TEM shows that most pores occur as spaces between subgrains, and particularly where three or more subgrains touch (Fig. 6; Worden *et al.*, 1990, Fig. 7). They also occur where bands or 'seams' of recrystallized feldspar abut against unrecrystallized material (Waldron and Parsons 1992, Fig. 8C,D; Waldron *et al.*, 1993, Fig. 2). Some pores (such as that illustrated by Waldron and Parsons, 1992, Fig. 8D) appear to be the cause of modification of texture in their vicinity. We conclude that micropore and subgrain formation are generally intimately connected processes.

Role of fluids

Roedder and Coombs (1967) and Sprunt and Brace (1974), who did not study the intra-feldspar textures, suggested that the micropores were the site of primary fluid inclusions (i.e. residual fluid trapped during original crystallization: Roedder, 1984). Sprunt and Brace (1974) suggested that bridges within micropores were developed during modification of original fluid inclusions in the presence of water at low temperatures. If fluid interacts with a curved pore it will start to dissolve feldspar at (curved) surfaces with high surface-energy and reprecipitate it on crystal faces with low Miller indices, and hence lower surface-energy (Roedder, 1984). This may in part be the cause of overgrowths in alkali feldspars.

Fluid is sometimes demonstrably present, using conventional fluid-inclusion microscopy (Roedder and Coombs, 1967), although pores in alkali feldspar are almost always too small for this type of work. Gases released from feldspars by laser-probe ablation or by room-temperature, *in vacuo* crushing, also reside to a large extent in micropores (Burgess *et al.*, 1992; Burgess and Parsons, 1994), although some of this loosely retained gas may reside in sites such as subgrain walls (Foland, 1994). As noted above, some pores appear not to affect the strain-controlled exsolution microtexture, indicating high-temperature trapping (Burgess *et al.*, 1992). The very vulnerability of elastically strained, coherent intergrowths to recrystallization at low temperature means that they are reliable markers of high-temperature trapping in feldspars. Fluids in turbid parts of feldspars may be different in origin (Burgess *et al.*, 1992) and may have a composition clearly indicating interaction with crustal rocks (Burgess and Parsons, 1994). Oxygen isotope work such as that of Ferry (1985) shows the interrelationship of turbidity and interactions with meteoric fluids.

The role of fluids in the development of irregular, coarse perthites from regular micro-or cryptoperthites illustrated by Parsons (1978) and Parsons and Brown (1984) is strictly circumstantial, but has been accepted implicitly by numerous workers (Ferry 1985; Parsons *et al.*, 1988; White and Barnett, 1990; Worden *et al.*, 1990; Guthrie and Veblen, 1991; Burgess *et al.*, 1992; Burgess and Parsons, 1994). The TEM work of Worden *et al.* (1990), Guthrie and Veblen (1991), Waldron *et al.* (1993) and Lee *et al.* (1995 and in prep.) and experimental work on $KGaSi_3O_8$ by Göttlicher and Kroll (1990) and on $KFeSi_3O_8$ by Walker (1991) is consistent with pervasive dissolution–reprecipitation as the mechanism by which the deuteric coarsening occurs. Oxygen isotopic work (Ferry, 1985) confirms that exchange occurs simultaneously. It seems that it

is during this stage that the pores develop, at points where subgrains meet.

Driving force

O'Neill and Taylor (1967), on the basis of experiments involving simultaneous oxygen and alkali exchange in feldspars, postulated reaction *via* a series of minute solution-redeposition steps in an advancing fluid film. In this case recrystallization occurred in the feldspar as a result of marked bulk chemical change. In natural feldspars crystal bulk compositions usually remain essentially constant during most deuteric reactions and two driving forces for recrystallization have been suggested by Brown and Parsons (1993), collectively called 'unzipping' processes. Elastic strain-energy stored in coherent cryptoperthites is large, up to $\sim 2.5-4$ kJmol^{-1}; reduction in free energy by this amount will occur when strain-controlled intergrowths recrystallize to coarser, largely incoherent, intergrowths. The formation of pores during this type of reaction was illustrated by Worden *et al.* (1990) and Waldron and Parsons (1992). A second driving force is provided by the loss of strain energy in the 'tweed' orthoclase domain texture, up to $\sim 2-3$ kJmol^{-1}, which transforms into 'tartan' twinned microcline. An example of the formation of micropores in conjunction with this reaction was illustrated by Waldron *et al.* (1993).

Volume reduction or mass transfer?

Although the evidence for extensive recrystallization within common alkali feldspars is strong, this in itself will not lead to pore formation because feldspar is also the product phase. Either volume reduction or mass transfer is required. During cooling from temperatures above the alkali feldspar solvus, volume reduction will take place for two reasons in addition to thermal contraction. Firstly, alkali feldspar solid solutions have a positive volume of mixing. For a bulk composition of $Ab_{15}Or_{85}$ (typical of subsolvus granites) the change in volume caused by unmixing is 0.5% (using cell parameters given in Smith and Brown, 1988, p.151). Secondly, a further small reduction will take place when ordering occurs in the, now separate, Ab and Or phases. This will account for a 0.04% reduction in volume on transformation from sanidine to microcline and a 0.45% reduction in volume on transformation from high to low albite (Smith and Brown, 1988, p. 140). This will lead to a total reduction in volume for the whole crystal of around 0.6%. There will also be a small volume change in each phase of the perthites resulting from loss of coherency (Tullis, 1975; Tullis and Yund, 1979). These will vary in a complex way with the bulk composition, coarseness and exact nature of the coherent microtexture, but will, in general, be negative for minor amounts of albite in potassium feldpar (as in the example from Shap), or positive for minor amounts of potassium feldspar in albite. In hypersolvus feldspars from syenites and high level granites (typically $Ab_{60}Or_{40}$) the total volume change will be larger ($\sim 1.3\%$). This change is not enough to account for the local microporosity of many feldspars and some feldspar material must be removed during the dissolution–reprecipitation process producing the micropores.

In deuteric perthites, micropores in the Or-rich phase are smaller, but more numerous, than those within the Ab phase. In many patch perthites in hypersolvus igneous rocks the Or-rich phase is substantially more turbid than the Ab-rich phase. We are uncertain as to the reason for this. The most probable explanation is that subgrains in Or-rich feldspar tend to be more stable than in albite because of the great textural variability of the orthoclase and irregular microcline mixtures of which which most deuterically altered K-feldspar is composed. Out-of-step boundaries will persist during prolonged fluid–feldspar reactions. In contrast, albite usually has a simple Albite-twinned microtexture and unless the angular misfit between subgrains is substantial (e.g. Worden *et al.* 1990, Fig. 7B), subgrain walls may readily anneal.

Porosity and permeability

The porous microtexture in alkali feldspars is permeable to fluids, but it can also, in places, retain them. Walker (1990) showed micropermeability to fluids experimentally by reacting partially turbid cleavage fragments with $H_2{}^{18}O$ for 75 h at 700°C, 0.1 GPa, and then imaging ^{18}O distribution by ion microprobe. High concentrations of ^{18}O were located in zones a few μm thick at crystal boundaries and also in microporous volumes at least 50 μm inside the crystal. These high concentrations within the crystals imply extremely high rates of fluid flow through the crystals, on the order of 5 km Ma^{-1}. In contrast, the $^{39}Ar/^{40}Ar$ method can be used to show that turbid feldspar, not only loses radiogenic ^{40}Ar through geological time (Parsons *et al.*, 1988), but also retains Ar (and halogens) in fluid inclusions, some of which contain primary magmatic fluids (Burgess *et al.*, 1992). This apparent contradiction seems likely to be related to the shape of each pore and the microtexture immediately surrounding individual pores. The importance of the shape of intercrystalline pores in crystal-melt assemblages was conveniently reviewed by Hunter (1987) and some factors are relevant to the intracrystalline (and inter-subgrain) pores considered in the present paper.

Pores with simple, crystallographically controlled shapes (e.g. Fig. 1B) are probably sealed, as the feldspar–feldspar–fluid dihedral angle is large. Pores with boundaries convex towards the fluid often have extremely pointed corners where the two opposite faces of a pore unite in a cusp (Fig. 1C). The TEM shows that such thin corners are defined by the surface between two feldspar subgrains. Provided the two-dimensional feldspar–feldspar–fluid dihedral angle approaches zero (as appears to be the case in many pores of this type), fluid will wet cracks between subgrains, and the feldspar will be permeable to fluids because an interconnecting fluid film will be present. In a rock containing a pore fluid, with separate mineral grains and substantial intercrystal, structural, angular misfit, this situation would lead to disaggregation. Subgrains in feldspar may have negligible misfit, or misfit brought about by opposite senses of order and antiorder in adjacent twins. Subgrain walls can be discontinuous and the feldspar therefore does not disaggregate. Where three adjacent subgrains are in contact, fluid will be continuous along subgrain edges only when the dihedral angle of the pore exceeds 60°. In effect this means that pores which are convex-out (towards the feldspar) will be sealed whatever the surrounding microtexture, while pores with convex-inward shapes, and cusp-shaped corners, are likely to be leaky and connected to neighbouring pores.

Geological and geophysical significance of micropores

Micropores make up a non-trivial proportion of most alkali feldspar crystals, which in turn are a major constituent of the continental crust. Although pores may retain fluid (Burgess *et al.*, 1992, Burgess and Parsons, 1994), they may also be markers of a permeable microstructure (Worden *et al.*, 1990; Walker, 1990). This permeability enormously reduces the effective grain size for volume diffusion in feldspars, and also increases the effective surface area. The pores and associated subgrain mosaic thus play an important role in many reactions involving alkali feldspar. Several geological situations and techniques to which they are relevant are summarized below. The microtextures may affect the way in which feldspars deform, and possibly influence the seismic and electrical properties of the crust. More detailed treatments of several of these applications have been, or will be, provided elsewhere.

$^{39}Ar/^{40}Ar$ dating and 'thermochronometry'

Because of their abundance and high concentration of ^{40}K, potassium feldspars are obviously strong candidates for application of the K-Ar dating method. A recent review was provided by Foland (1994). It soon became clear to pioneers in this field that K-feldspars from plutonic rocks were usually unsatisfactory for dating purposes, either because they gave geologically unreasonable, young apparent ages, indicating Ar-loss, or unrealistically old ages indicating the presence of 'excess' Ar. The related $^{39}Ar/^{40}Ar$ step-heating method provided a partial solution to this problem and the diffusive loss of Ar has been turned into a virtue by Harrison and co-workers (e.g. Lovera *et al.*, 1989, 1990) who have developed methods reputed to give an insight into the thermal history of any suitable sample, so-called 'thermochronometry'. Some remarkable claims have been made for this method (e.g. Richter *et al.*, 1991), although other workers, such as Villa (1994), have argued that the technique is theoretically flawed. Developments of the technique (Lovera *et al.*, 1989, Harrison, 1990) imply that alkali feldspars have a 'multidomain' texture, as far as Ar-release is concerned, with diffusion 'domains' considerably smaller than the dimensions of the crystal; micro-textural features corresponding with the 'domains' postulated by analysis of step-heating spectra have not yet been clearly identified (Fitz Gerald and Harrison, 1993).

The importance of microporous texture in $^{39}Ar/^{40}Ar$ work has been demonstrated and discussed in a number of papers (Parsons *et al.*, 1988, Burgess *et al.*, 1992, Burgess and Parsons, 1994). Although some workers were initially doubtful of the role of micropores (Lovera *et al.*, 1989, Harrison, 1990, Foster *et al.*, 1990) it is now clear that pores are a repository of loosely retained Ar, sometimes comprising a significant part of the 'excess Ar' component. This factor is particularly important when laser-ablation techniques for argon release are attempted because ^{40}Ar from fluid inclusions may be released from a volume of sample considerably larger than the laser beam, leading to anomalously old apparent ages. Argon, and also isotopes derived by neutron reactions with trapped halogen-bearing fluids, can be released from feldspar by simple *in vacuo* crushing experiments (Burgess *et al.*, 1992, Burgess and Parsons, 1994). Harrison *et al.* (1993) have suggested that argon in fluid-inclusions may be unimportant in some applications of the step-heating method.

The subgrain texture which commonly occurs together with micropores is unquestionably important in argon loss (Parsons *et al.*, 1988) and is likely to provide a range of 'diffusion domain' dimensions. The spaced dislocations on semicoherent exsolution lamellae (Waldron *et al.*, 1994, Lee *et al.*, 1995) also provide likely pathways for comparatively rapid Ar transport. The boundaries of fully coherent lamellae do not provide pathways for Ar loss (Parsons *et al.*,

1988). It remains to be seen whether these features can be correlated with the diffusion domains predicted by the methods of Lovera *et al.* (1989, 1990) and it is also essential to understand the stability and behaviour of the textural features during $^{40}Ar/^{39}Ar$ step heating. For practical thermochronology, the time–temperature evolution of the microtextures must be known. At present the models assume that the microtextural features are present throughout the entire cooling history of each feldspar, whereas we have demonstrated above that the microporous texture often develops at $T \leqslant 400°C$ and modification may continue to surface temperature. The sub-regular dislocations which occur in Or-rich micro- and cryptoperthites (Waldron *et al.*, 1994, Lee *et al.*, 1995) will form over a range of temperatures, as the structure stiffens, depending on the local bulk composition of the feldspar and the cooling rate. Deuteric alteration of microperthites demonstrably postdates the formation of dislocations (Fig. 7). It is not obvious whether turbidity in feldspars will develop during a simple, monotonic, cooling process or later and perhaps repeatedly. This is likely to be a serious complication in the synorogenic granitic intrusions studied, for example, by Richter *et al.* (1991). The closure temperature, which is a function of the square of the effective diffusion dimension (Dodson, 1973), is a feature which evolves with time in feldspars. Furthermore, the microtextures controlling diffusion in nature must remain unmodified during the laboratory heating experiment. In addition to the theoretical problems described by Villa (1994), these questions of the temporal stability of the crucial microtextures seem to us to raise serious doubts as to whether argon step-heating spectra can be inverted to provide thermal histories (see also Brown and Parsons, 1994).

For comparatively simple, anorogenic intrusions, it is certainly possible to make qualitative deductions concerning thermal history, and to place limits on thermal events that a sample may have experienced. For example, a sample of microporous feldspar in the 1166 Ma Klokken intrusion (Parsons *et al.*, 1988) had lost nearly 45% of its radiogenic ^{40}Ar (integrated age 662 Ma), whereas an adjacent sample of pristine feldspar was very retentive (integrated age 1126 Ma). Consideration of effective diffusion dimensions estimated from TEM work (Worden *et al.*, 1990) allowed Burgess *et al.* (1992) to suggest that loss from the porous feldspars could be accounted for by sustained heating at $\leqslant 150°C$ since the Proterozoic and precluded any short-lived thermal events at $T \geqslant 240°C$ at any time. In contrast, Burgess and Parsons (1994) showed that highly altered, microporous feldspar in the Tertiary Loch Ainort granite, Skye, had retained almost all its ^{40}Ar, suggesting that the intrusion cooled rapidly to surface T, and remained cool subsequently.

Oxygen exchange

Feldspars frequently continue to exchange oxygen down to low temperatures and are often the last mineral to close to oxygen exchange in multiphase assemblages (Giletti, 1985). Giletti discussed the processes by which oxygen isotopes may exchange in minerals. These are volume diffusion and exchange accompanied by dissolution and reprecipitation, either without bulk chemical change, as for a rock undergoing deformation, or as part of a solid–fluid reaction in which the composition of the solid changes (as in the experiments of O'Neill and Taylor, 1967, recalled above). ^{18}O–^{16}O exchange to achieve isotopic equilibrium does not in itself provide an adequate driving force as free energy changes are miniscule. There is a considerable literature on volume diffusion of oxygen in feldspars (reviewed most recently by Giletti, 1994, and Graham and Elphick, 1994). There has been disagreement in the past as to whether experimental exchange was by diffusion or by surface reaction but there is a general consensus that the careful experiments of Farver and Yund (1990), which show that oxygen diffusivities are strongly dependent on water fugacity, represent volume diffusion through an undisturbed structure. An absolutely rigorous demonstration, ruling out infiltration along sub-optical pathways, such as those described elsewhere in the present paper, would require before-and-after TEM work and this has not been done. It would be extremely interesting to know whether oxygen diffusion can occur through an elastically strained structure, such as coherent cryptoperthite or tweed orthoclase, at low temperatures, without loss of coherency. The experimental work implies that O diffusion at $T < 500°C$ is faster than that of the alkali cations, with a much lower activation energy.

Whatever the mechanism at high temperatures, the textural evidence for extensive solution–reprecipitation in alkali feldspars at lower temperature is incontrovertible. Textures such as those shown in Fig. 6 clearly result from growth of new feldspar. As explained by Brown and Parsons (1993), release of coherent, elastic, strain-energy provides a driving force independent of externally imposed strain. It is reasonable to conclude that recrystallization occurred through the medium of a fluid that penetrated deep into the interior of crystals, in this case facilitated by dislocations at semicoherent microperthite interfaces. The textural hallmark of these reactions is the development of subgrains with the {110} Adularia habit, often with micropores between them. The oxygen isotope ratio of the affected volumes is

probably set during the reprecipitation process; laser-probe oxygen isotopic techniques may soon have the resolution to establish contrasts between pristine and deuterically altered texture. Microporous feldspar, once formed, is clearly permeable (Walker, 1990); oxygen exchange may occur by volume diffusion into existing subgrain textures, or by new growth and rearrangement within such textures, as illustrated by Worden *et al.* (1990, Fig. 7C).

Although exact spatial correlation of $\delta^{18}O$ distribution with microtextures cannot yet be achieved, a general correlation with turbidity in the Tertiary granites of Skye was established by Ferry (1985) and the textural changes at the TEM scale were illustrated by Guthrie and Veblen (1991). In this instance, the aqueous fluids came largely from envelope rocks (Taylor and Forester, 1971; Burgess and Parsons, 1994). $^{39}Ar/^{40}Ar$ work in the latter study suggested that, once the porous textures formed, the feldspars cooled rapidly to surface temperatures and were not further modified. In contrast, the pervasive textural changes in the laminated syenites of the Klokken syenite (Worden *et al.*, 1990) resulted from interactions with a fluid of magmatic origin ($\delta^{18}O_{SMOW}$ 3–8‰, Parsons *et al.*, 1991). Worden *et al.* (1990) speculated that this fluid exsolved from the feldspars, following a suggestion in Brown *et al.* (1983). Subtle, sub-optical solution-redeposition and pore development was illustrated by Waldron *et al.* (1993) in mildly retrogressed granulite facies rocks and this could potentially be accompanied by change in $\delta^{18}O$ without textural modification at the optical scale.

Rb and Sr diffusion

Giletti (1991) provided data for Rb and Sr diffusion in K-feldspar and albite, and discussed the application of these data for deduction of closure temperatures and hence the cooling histories of rocks. Many of the factors discussed in the preceding two sections are again relevant. Giletti correctly discussed the importance of microtexture (for which he cites what is implicitly semi- or in-coherent perthite) in controlling the effective diffusion dimension, and mentioned the problem of the temperature evolution of the microtextures. However, the textures described in the present paper form at or below the closure temperature for normal crystal sizes in a plutonic granite even at cooling rates as low as 0.1 KMa^{-1} and microporous subgrain textures of the dimensions described in the present paper will have extremely low closure temperatures ($\ll$ 300°C) if they are in equilibrium with a suitable reservoir. As with oxygen exchange, microporous K-feldspar effectively provides a reactive reservoir of Rb and Sr with which other phases, which close at higher T, may exchange *via* a fluid phase. Solution-reprecipitation will clearly reset both Rb and Sr at low T in alkali feldspars, and potentially permit modification of apparent $^{86}Sr/^{87}Sr$ initial ratio if reaction is with an extraneous fluid. Although no analytical technique exists at present with the resolution needed to correlate possible redistribution of these elements exactly with microtexture, ion-microprobe work (Walker, 1991) has shown qualitatively that much greater internal variability exists in analyses in microporous regions than in adjacent pristine parts of crystals. It is, however, difficult to disentangle the effects of redistribution that accompanies the coarsening of perthite from bulk changes that are induced by fluid–feldspar reaction.

Weathering

Naturally weathered and artificially altered feldspar grains have extremely irregular surfaces covered by what are usually called etch-pits (e.g. Tchoubar, 1965; Seifert, 1967; Lundström, 1974; Wilson, 1975; Berner and Holdren, 1977, 1979; Keller, 1978; Nixon, 1979; Holdren and Berner, 1979; Eggleton and Buseck, 1980; Helgeson *et al.*, 1984; Lasaga and Blum, 1986; Velbel, 1986; Aldahad and Morad, 1987; Murphy, 1989; Tazaki and Fyfe, 1987). The early weathering of phenocrysts from the Shap granite is described in detail by Lee and Parsons (in press). As weathering proceeds, shallow, curved or irregular pits become deep, angular and 'prismatic' in shape. In highly dissolved grains the pits coalesce, leading to delicate skeletal relics.

All surface pits on the μm-scale have generally been assumed to be weathering products produced by selective dissolution around lattice-scale reactive sites. Eggleton and Buseck (1980), for example, used TEM to illustrate the development of 'negative-crystal' micropores from precursors with circular cross-section which they suggested had nucleated on regions of high strain at the ends of Albite twin lamellae. Helgeson *et al.* (1984) suggested that etch-pits formed by the 'autolocation' (Boldryev, 1979) of dislocations. They discussed the contribution of the core and strain energy of dislocations, spaced on the order of 1μm apart (10^6 dislocations mm^{-2}), to the activation energy of dissolution, and concluded that the distribution of such dislocations on the feldspar surface was the main control of dissolution rates. Lasaga and Blum (1986) treated the mathematics of etch-pit formation in general using a Monte Carlo method to simulate the development of etch-pits from screw dislocations, that were stated to occur in the density range 10^2–10^8 mm^{-2}. Inputs to their model are the degree of undersaturation of the aqueous solution with respect to the reactant mineral, the shear modulus of the mineral, surface tension, molecular volume, and the Burgers vector and

radius of the dislocation core. The simulated shape of the etch-pit was determined by the degree of undersaturation, low undersaturation leading to narrow, hollow cores along the dislocation line, high undersaturation to widespread dissolution and the formation of proto-etch-pits. Meike (1990) has recently suggested that the variation in strain energy associated with the microstructural detail of dislocations may be of the same order as that associated with dislocation density, so that the detailed character of dislocations, and not merely their density, must be considered. Lee and Parsons (in press) have shown that weathering is extremely rapid around dislocations on perthite lamellae in the Shap granite (similar to the laboratory dissolution illustrated in Fig. 7), leading to the rapid development of tubular etch pits >15 μm long and a few tens of nm cross section. Experimental studies explicitly concerned with the role of dislocations in controlling dissolution rate, in which dislocations were experimentally induced by deforming the starting materials, were reported by Holdren *et al.* (1988) and Murphy (1989). Nesbitt *et al.* (1991) correctly suggested that it is the concentration of dislocations around exsolution lamellae that causes dissolution to be concentrated in these areas. While this is true, it seems that many micropores have often developed in such regions prior to weathering (Fig. 7), as suggested by Fung *et al.* (1980).

As discussed above, dislocations in semicoherent microperthites commonly form planar arrays. Spacings range from <100 nm (Brown and Parsons, 1984) to 1400 nm (Aberdam, 1965), rather less than those proposed by Helgeson *et al.* (1984). These dislocations readily etch in HF (Fig. 7), and also in water (Wilson and McHardy, 1980; Lee and Parsons, in press) and are likely to evolve into etch-pits. However, the density and irregularity of distribution of 'etch-pits' on weathered surfaces suggests that the majority are actually developed from micropores formed during cooling of the original igneous or metamorphic rock, and are not related to individual dislocations. The density of original micropores (Table. 1) is comparable to that proposed in the theoretical treatments of Helgeson *et al.* (1984) and Lasaga and Blum (1986). In extreme cases, naturally weathered feldspars form delicate skeletal structures. As noted earlier, micropores are not evenly distributed through crystals but are restricted to areas of coarsened perthite, which often form bands. This distribution of micropores, together with preferential dissolution of dislocation arrays on perthite lamellae, may contribute to the uneven distribution of the effects of weathering in experiments and natural situations, the pristine structure (e.g. the comparatively featureless volumes with small exsolution lamellae without dislocations on Fig. 7), leading to the relatively resistant elements in the skeletal frameworks.

Experimental dissolution

The literature on experimental dissolution of feldspars is large. A recent review was provided by Blum (1994). As in natural weathering, a major effect will be the large increase in surface area. Blum provided a table comparing geometrical surface area, calculated for sets of sieved fragments, with surface area measured by the BET gas adsorption method. The latter is always larger in alkali feldspars, by a factor of between 14 and 3, called the 'surface roughness' (SR). Weathered feldspars in soils commonly have SR of several hundred. In plagioclase feldspars the SR may be as large as 130, and is commonly larger than in alkali feldspars. Measurements of SR by Atomic Force Microscopy indicate SR of only ~2 (Blum, 1994), so that the enhanced surface area must be internal to the crystals. Pores connected by subgrain boundaries and dislocations can all potentially contribute to enhanced surface area over that defined by simple grain geometry. Gases used in the BET method (N_2 and Kr) have small molecular diameters (~0.4 nm) so that many of the irregularities described in the present paper will contribute to the BET measurements. It is not clear to us why some plagioclases have such large values of SR and it would be valuable to characterize them with SEM and TEM. Electron microscopy should be mandatory for any feldspar whenever relative dissolution rates are measured and it would be valuable to compare BET and dissolution-rate measurements on pristine and turbid material of the same bulk composition.

Development of secondary porosity and diagenetic albitization.

Micropores will play a role in diagenesis similar to that in weathering and surface dissolution, although the fluids are likely to be of a different composition (e.g. Bevan and Savage, 1989; Manning *et al.*, 1991). Dissolution rates will be enhanced, leading to development of secondary porosity by partial or complete removal of microporous alkali feldspars. In clastic sequences with restricted source regions, the rate of dissolution of feldspar, with dependent evolution of pore-fluid composition, and precipitation of clays, might ultimately depend on the microporosity of feldspars in the igneous or metamorphic source. If dissolution occurs in fluids of the appropriate composition, it may be followed by diagenetic albitization of the original grain (Saigal *et al.*, 1988; Aagaard *et al.*, 1990). The SEM micrographs in Saigal *et al.*, showing small

(1–30 μm) albite grains developing within detrital K-feldspars, seem entirely consistent with prior leaching of originally microporous grains with subsequent precipitation of albite. It is an extreme development of the type of new feldspar growth found in micropores in feldspars from igneous rocks (Worden *et al.*, 1990, Fig. 7C). Saigal *et al.* studied albitized grains forming at known down-hole temperatures and found this style of replacement at 65–90°C. They were unable to reconcile the preferential dissolution of K-feldspar with the observation that some parts of grains appeared to be resistant to replacement. Original crystals with normal patchy or banded development of inherited microporosity provide an excellent explanation.

Leachable sources of metals

The concentration of ore-forming metals by precipitation from low-T epigenetic hydrothermal solutions is an established process in the formation of carbonate-hosted, Mississippi Valley-type ore deposits. Flushing of metals disseminated in microporous feldspar provides a possible source. A more direct and testable connection may exist in 'porphyry'-type copper, molybdenum and tin deposits, which are characterized by zones of variable alteration, often extreme, in the host granites. It would be interesting, although rather difficult and time consuming, to relate the character of metallic inclusions in micropores in the least altered feldspars to the concentrations of metals developed in the mineralized parts of the porphyry system.

Nuclear waste isolation

Once radionuclides have escaped a repository and reached the country rock, the speed and concentrations with which they reach the biosphere are controlled by the rate of the fluid flow and the physical and chemical environment along its path; in particular the ability of the rock to retard the movement of the radionuclides (Rickert *et al.*, 1979; Chapman and McKinley, 1987). Retardation can be brought about by the process of 'dead-end diffusion'. Water flowing through a system of fissures is in contact with void space which is essentially static, e.g. dead-end cracks leading off the main fracture and intragranular porosity. Dissolved radionuclides will be able to diffuse down concentration gradients into these pore spaces and cannot move back into the main flow other than by diffusion which would require a reversal of the concentration gradient. Much work in this field (Neretnieks, 1980; Grisak and Pickens, 1980; Bradbury and Green, 1986) indicates that this could be a very effective means of retarding escape of radionuclides. It might be expected that, by increasing the amount of dead-end pore space available, interconnected micropores would increase the potential of a feldspar-bearing rock to retard radionuclides (E. Roedder, pers. comm., 1990). Feldspar-rich rocks with turbid feldspars might therefore form better repositories than less altered rocks.

Deformation

The response to natural and experimental stress of microporous and pristine feldspar is likely to be different, since feldspar which is undeformed but normally microporous also has a high concentration of dislocation arrays, subgrain boundaries and cracks leading into micropores. There have been a large number of papers on the experimental deformation of feldspars and feldspar-bearing rocks, reviewed most recently by Smith and Brown (1988). The general conclusion is that at $T \leqslant 600$°C deformation occurs by fracturing but at higher temperature deformation occurs by dislocation glide. The microtextures in alkali feldspars described in the present paper form spontaneously in the absence of stress at temperatures well inside the fracture regime. Fracture mechanisms in general were summarized by Atkinson (1982) and more recently by Lloyd and Knipe (1992). It seems highly probable that microporous subgrain textures have a critical role in determining the relative importance of intragranular and intergranular fracture in feldspar-bearing rocks, and turbid feldspar should have a considerably lower fracture stress than pristine feldspar. Spaced dislocations at perthite interfaces may also serve to nucleate fractures. The 'Murchison plane' of easy fracture is not a true cleavage plane, but is defined by an orthogonal net of intersecting dislocations, one parallel to b, in the plane $(\bar{6}01)$. Fluid inclusions and fluid films at subgrain boundaries are likely to be important in subcritical crack propagation (stress corrosion) (Atkinson, 1982). Indeed it might be argued that the subgrain boundaries are a category of subcritical crack in that they form and propagate by dissolution and reprecipitation. The driving force for their formation is internal elastic strain energy (Brown and Parsons, 1993) and external stress is not necessarily involved, but the textures which result are similar to those produced by deformation (e.g. Worden *et al.*, 1990, Fig. 7B).

In crystals that have 'dual microtexture' (Brown and Parsons, 1994) deformation mechanisms are likely to vary substantially from place to place, even within a single crystal. In nature the normal population of subgrain boundaries and dislocations in undeformed feldspar will be strongly temperature-dependent. Tullis and Yund (1977) studied the deformation, under 'dry' conditions, of the subsolvus

granite from Westerly, Rhode Island, that has been used for numerous studies of crack propagation at 25°C (see Atkinson, 1982), and which continues to be used for deformation and melting studies (Neumann and Rutter, 1994). According to Tullis and Yund, TEM examination of undeformed Westerly granite revealed 'very few dislocations' (in quartz, plagioclase and alkali feldspar), but the high-quality, optical micrograph of this rock given by Tuttle (1952, Plate 3) clearly shows that alkali feldspar is at least somewhat turbid, and plagioclase is extremely so. While it may be true that dislocations are few in pristine feldspar, it seems highly probable that pores and subgrain textures abound in the turbid feldspar that makes up a significant volume of the rock. When deformation experiments of normal duration are carried out on rocks with turbid feldspar at T above that at which the subgrain textures form in nature (perhaps <350°C, see section above; Tullis and Yund worked between 25 and 1000°C, 0.15–1.5 GPa) the sample under investigation will have a considerably different microtexture from that which it would have possessed in the crust at the same temperature. At temperatures above the solvus it will also be considerably different in terms of its exsolution microtextures unless the experiments are sufficiently long to cause homogenization of perthite. Spaced dislocations at semicoherent interfaces will form at sub-solvus temperatures, depending on local bulk composition and cooling rate. Their behaviour during rapid reheating is unknown. Tuttle (1952) considered the textural evolution of Westerly granite in some detail and concluded that some of the albitic plagioclase exsolved from orthoclase and then migrated to boundaries between orthoclase and plagioclase. Thus, experiments on this rock at elevated temperature involve an assemblage of feldspars that is both chemically and texturally metastable. The abundance of fluid-filled pores in alkali feldspar (and their more obvious presence in quartz) also raises the question of whether deformation experiments are ever truly 'dry'. It seems to us certain that deformation experiments on granitic rocks taken rapidly to elevated temperatures are highly unrealistic in terms of microtexture. The role of pre-existing microtexture in the response of feldspar to stress would repay close investigation.

Seismic anisotropy

Seismic shear-waves in the upper crust almost always exhibit shear-wave splitting, caused by the elastic anisotropy that is common to a large range of igneous, metamorphic and sedimentary rocks (Crampin and Lovell, 1991). Although the wavelengths of the shear waves showing anisotropy are extremely long, >1m to <1km, the anisotropy is probably caused by cracks on the scale of a few μm to a few m (Crampin and Lovell, 1991). The observed anisotropy may be modelled satisfactorily on the basis of thin, isolated, coin-shaped, fluid-filled microcracks aligned perpendicular to the minimum regional compressional stress. These are known as EDA-cracks (extensive-dilatancy anisotropy). The real shape of the features is no doubt more complex, but the statistical averaging provided by the relatively very large seismic wavelength ensures that the features causing the anisotropy can be represented by relatively simple cracks. The μm scale of the smaller features is considerably less than the crystal size in all deep-seated crustal rocks and, in view of the preponderance of feldspar in the crust (>60 vol.% in granites), fluid-filled micropores and associated microcracks could be the features at the lower end of the scale range. However, this will be true only in the upper crust where temperatures are less than the temperatures of formation of pores (i.e. <400°C). It might be possible to establish, using samples whose orientation relative to the regional compressive stress is known, whether cracks and pores orientated in the appropriate direction are more open than others. In the Moine (Proterozoic) metamorphic rock studied here (Fig. 1F) micropores were elongate and strongly orientated, but overall, seismic anisotropy reflects the present-day regional stress, so there would need to be preferential dilation of such features normal to the current compressive stress.

The distribution of cracks in rocks is known to be fractal (Leary, 1991). This means that fractures are self-similar over a wide range of scales, with larger fractures associated with a multiplicity of smaller fractures. As with a coastline, cracks become more complex the closer they are inspected. Cracks tend to cluster in space; thus major fractures, such as faults, are associated with minor splays and also with cracking down to the grain scale. Between these major zones of fracturing are volumes of rock which contain only comparatively small cracks. It is the latter cracks that exhibit the preferred orientation that accounts for seismic anisotropy. Our observations show that in alkali feldspars this fractal character continues to well below the scale of the individual crystal. Crack systems such as those shown in the present Fig. 6, and by Worden *et al.* (1990, Fig. 7B) are similar to the grain texture of the rock but are intracrystalline. Furthermore, the intracrystal subgrain boundaries with spacings on the μm-scale are clustered, often forming bands across crystals that surround volumes of comparatively crack-free, pristine texture on the mm scale. As the smallest subgrains we have observed have dimensions of only a few tens of unit cells, the subgrain boundaries must represent the lower limit of the fractal character of cracks in rocks.

Another interesting feature of crack distributions is the inference, from seismic anisotropy, that the crack sizes vary very little between essentially intact rock and heavily fractured rock, even though crack dimensions inferred from intact igneous rocks (μm–mm) and unstable fractured rock (m to many m) appear to cover a very large range. Crampin and Leary (1993) considered that this implies that much of the crust is in a state close to fracture criticality, where a small increase in crack density will rapidly lead to the development of continuous, through-going fractures, and a transition to heavily fractured, disaggregated rock. This seems to describe the microcracks and porosity we see in feldspars rather well. The Ar-loss work (Burgess *et al.*, 1992; Burgess and Parsons, 1994) implies that some fluid inclusions in feldspars remain sealed for long periods of geological time, whereas others may suffer steady leakage of radiogenic Ar (Burgess *et al.*, 1992). Thus crystals contain regions of separate, unconnected cracks and pores, together with regions in which cracks extend to the crystal surface. Worden *et al.* (1990) commented that the distribution of turbid material within feldspars suggested a sudden process 'triggered' erratically in some parts of crystals rather than others, and this might correspond with a rapid advance of recrystallization once a critical crack density is reached. Although the main thermodynamic driving force for recrystallization in alkali feldspars seems to be coherent elastic strain energy and is independent of external stress, it is certainly possible that the process may be localized by external stress, caused, for example, by differential thermal contraction in a polymineralic rock.

Electrical conductivity

Deep electromagnetic sounding methods show that the middle to lower continental crust is more electrically conducting than is suggested by experimental measurements of the conductivity of likely lower crustal rocks measured at surface temperature and pressure. Recent reviews are by Jones (1992) and Frost and Bucher (1994). Whereas laboratory measurements of electrical conductivity of rocks and minerals give resistivities of 10^3–10^5 Ω m, estimates of the resistivity of the lower crust using the magnetotelluric method suggest values often $<10^2$ Ω m. The exact shape of this conducting zone is not well defined and it is not possible to tell whether the zone is comparatively thin and highly conducting, or moderately conducting, but thicker. Nevertheless, there seems to be agreement that conductivity increases sharply at mid-crustal depths around 15–20 km, provided temperature is >350–400°C. Explanations include the presence of brines, graphite films, partial melting and the presence of conducting minerals, particularly magnetite. Melting requires high temperature and it is not obvious why the lower crust, as we presently understand it, should be generally enriched in a conducting, major mineral phase such as magnetite. Thus, at present, the first two are the main contenders to explain the high conductivity.

Brines. In places, the conducting zones correspond with large-scale seismic reflectors, such as subduction zones, providing evidence that the presence of fluids does increase conductivity. Fluid films have therefore become the most favoured explanation of the high conductivity of the lower crust (e.g. Hyndman and Shearer, 1989), although many problems have been discussed by Frost and Bucher (1994). The most obvious problem is considered to be the difficulty of maintaining a separate aqueous phase because small amounts of water will be consumed by hydration of mafic silicates. However, quartz and alkali feldspar are stable in the presence of water up to the beginning of melting in granitic terrains and both are potential hosts for brines in fluid inclusions. Indeed, Burgess *et al.* (1992) have demonstrated the presence of halogen-bearing inclusions with 'mantle' Ar-halogen ratios in relatively rare pores in pristine feldspar. However such fluid inclusions will be isolated and may not contribute significantly to electrical conduction. On the face of it, microporous feldspar with a subgrain network including fluid films is an attractive explanation of enhanced electrical conductivity, but, unfortunately, the electrical conductivity of the crust appears to decrease at the temperature at which an interconnected microporous texture first develops. The correlation is, if anything, a negative one. However, in a burial situation it is probable that a microporous texture, once formed, would persist to substantially higher temperature. The presence of extensively microporous feldspar at depth in metamorphic terrains is thus a possibility. It would be valuable to compare the electrical conductivity of carefully dried and brine-saturated microporous feldspar, and also that of truly pristine, 'gem quality' feldspar. The remarkable time-dependent properties of the gem-quality sanidine from Volkesfeld, Eifel (Bernotat-Wulf *et al.* 1988), which was transported extremely rapidly from the deep crust, and which possibly contains a transient H species (Graham and Elphick, 1994), may be highly relevant to the *in situ* properties of feldspar in the deep crust.

Carbon films. Frost *et al.* (1989) and Mareschal *et al.* (1992) have presented interesting observations of C (as well as Cl and S) on grain surfaces in feldspathic rocks. They used Scanning Auger Spectrometry, which is sensitive to elements in the outer 6 nm of a surface. The diameter of the incident electron beam was ~1 μm and SEM images and

corresponding elemental maps were provided of areas about 200 μm in side. Frost *et al.* studied grain surfaces of crystals in two monzosyenites and a gabbroic anorthosite from the Laramie Anorthosite complex, and Mareschal *et al.* looked at surfaces in meta-tonalites, paragneisses and anorthosites from the Kapukasing uplift in the Canadian Shield, both sets of samples deemed to be representative of the lower crust. Although SEM micrographs of grain surfaces were supplied, it is not possible to identify, unequivocally, the mineral investigated. The authors state that the rocks were 'gently crushed', but they do not explain how they ensured that the surfaces under investigation were natural grain boundaries, or why some surfaces in the micrographs are considered to be grain boundaries, while others are not. However, the lithologies studied are such that the majority of grains are very likely to be feldspar. Traces of C were reported from Laramie, and C, Cl, and S from Kapukasing. Using an Ar-sputtering technique, the C was shown to be in a zone ~100 nm thick at Laramie and 30 nm in the Kapukasing anorthosite, and the Auger electron spectrum was identical to crystalline graphite. Traces of Cl and S were found to be 'sporadically' present. If the phases studied were indeed feldspar the question immediately arises: were the authors seeing material in near-surface micropores? Was it really a continuous film? The SEM micrographs provided are at far too low a magnification for micropores to be visible. As we have shown above, sub-μm pores containing particles are common, and although we have not encountered graphite, we have seen NaCl and sulphides.

If we accept that continuous graphite films are present between pristine feldspar grains at T >350°C in the deep crust, the development of microporosity offers a possible explanation for the breakdown of such films at lower temperatures in the upper crust. As we have argued above, microporosity results from feldspar–fluid interactions at <350°C and is accompanied by a marked breakdown in the structural continuity of the feldspar. Not only is oxidation likely, but even in rocks in which f_{O_2} was buffered to be in the stability field of carbon, breakdown of continuous surface films seems inevitable.

Outstanding questions

Some important questions can be asked with respect to porous microtextures. In particular we need to have a clearer view of the temperature range of their development. This is particularly important in isotopic work that relies on the concept of closure temperature. Some advances are likely as more evidence emerges from TEM work of the time relationships of coherent exsolution and deuteric textures. Some progress has recently been made (Waldron and Parsons, 1992; Lee *et al.*, 1995, in prep.).

It is also important to establish experimentally the thermal stability of the textures in regimes of increasing temperature. Do such textures seal during metamorphism and, if so, in what temperature range and at what rate? Although porous textures in granitic K-feldspars do not develop until <350°C during cooling, they may not disappear on heating at this temperature, because the crystalline phases (microcline or orthoclase and low albite) are stable to higher temperature, and until appreciable Si,Al disordering occurs, there is no chemical driving-force for large-scale textural change. Does behaviour vary between 'dry' and 'wet' regimes? Does fluid composition influence the stability of pores, their shape, and connectivity? These are non-trivial questions because the reactivity of feldspar, in the broadest sense and including isotopic exchange reactions, will change markedly if porous textures seal and anneal during heating. A more trivial, but still important, question concerns the stability of subgrain textures and spaced dislocations during $^{40}Ar/^{39}Ar$ step heating experiments. Rather limited experimental work to date (Fitz Gerald and Harrison, 1993, and papers reviewed in Foland, 1994) is far from conclusive on this issue. There are also questions connected with experimental work on the mechanical properties of feldspars. Do pores strongly affect their deformation behaviour? Do pores close normal to the direction of applied stress, and can they therefore account for seismic anisotropy? This might be answered by TEM investigation of carefully collected orientated samples. In the field of electrical conductivity measurements, a means should be sought of measuring resistivity of samples under conditions in which pore distribution, contents and geometry are those corresponding with chemical and textural fluid–rock equilibrium in the lower crust, and a more sophisticated approach to the character of grain surfaces, and possible conductive films, is needed.

Conclusions

Micropores, the majority on the scale of <1 μm, and the dislocations and subgrain boundaries which connect them, are a non-trivial feature of alkali feldspars. They, and their contents, are the main cause of the variable appearance of feldspars. Pristine feldspars (dark in colour in hand specimen) contain few pores, but these may contain fluids of deep-seated origin. Turbidity, developed to greater or lesser extent in almost all feldspars, is largely caused by micropores, which form typically 1–2 vol.% of the crystal, but may form up to 4.5 vol.%, at concentrations of up to 10^9 mm^{-3}. Pores develop

during the cooling of igneous and metamorphic rocks, usually in conjunction with loss of coherent elastic energy in crypto- and micro-perthites, and with release of strain energy in the tweed orthoclase texture during the orthoclase–microcline transformation. In many granitic rocks, the majority form at temperatures below 400°C, and, with the surrounding microtexture, may undergo further modification at near-surface temperatures, as in diagenetic albitization. Fluids responsible for low temperature alteration may be extracted from the pores. Some pores form at much higher temperatures and may trap primary igneous fluids. The minimum trapping temperature of such pores can deduced from the character of the enclosing microtexture.

The microporous and micropermeable texture accounts to a great extent for the exceptional low temperature reactivity of alkali feldspars and their ability to exchange oxygen isotopes to low temperatures. Experimental work shows that oxygen can be transported on the order of 5 km Ma^{-1} through the microporous texture at 700°C and 0.1 GPa. Rb and Sr will be reset, like O, by the common solution-reprecipitation reactions forming the micropores. Pores and subgrains have an important role in argon systematics. Leachability of feldspars will be enhanced by micropores, perhaps leading to dissolution of enclosed metal oxides and sulphide grains in hydrothermal solutions, and, ultimately, to their reprecipitation and concentration to ore grade. Micropores are an important control of the weatherability of feldspars, particularly its patchy character, and account for the rapid, but variable, development of skeletal forms during soil formation. They are likely to be a cause of the contrast between grain surface area calculated from grain geometry and that measured using gas adsorption, and must be a major reason for variations in dissolution rate observed for feldspars of similar composition in dissolution experiments. Pores are likely to be important in radioactive waste disposal in that they enhance the rate of reaction of feldspars with hot aqueous fluids, and also because the microtextures provide dead-end pore space for migrating radionuclides. The role of micropores, and the associated subgrain textures, in both natural and laboratory rock deformation should be explored. More speculatively, they may be an important factor in the anisotropy and attenuation of seismic signals in the crust, and may have a role in the variable electrical conductivity of crustal rocks.

Perhaps the most important lesson we have learned from this and associated TEM work is that feldspars in plutonic rocks crystallized at both shallow and deep crustal levels are almost always, to a greater or lesser extent, penetratively altered. They are profoundly different microtexturally, and possibly chemically, from the feldspar as it existed within a few hundred degrees of its crystallization temperature. This is true of most rocks considered 'fresh' by petrologists. The 'black' syenites and rapakivi granites which we regard as novelties may be much more representative of the igneous rocks of the middle and lower crust, observed *in situ*, without the modification which almost always attends uplift and exhumation.

Acknowledgements

We are grateful to John Findlay and Chris Jeffree of the Edinburgh University Science Faculty EM Unit for help in obtaining the SEM images, and to David Humes of the Department of Biochemistry for provision of TEM facilities. Ion probe work was done on the NERC-supported Edinburgh ion microprobe, under the supervision of John Craven. Our insights into microstructure were advanced enormously by collaboration with R.H. Worden (who took Figs. 6A and B) and K.A. Waldron, who were supported by NERC Research Grants GR3/6695 and 8374, and by constant interaction with Bill Brown, in Nancy, France, who also greatly improved an early version of the manuscript. Peter Leary, in Edinburgh, made helpful comments on our ideas in the realm of geophysics. F.D.L.W. was supported by NERC research studentship GT4/88/GS/1 and M.R.L. by NERC Research Grant GR3/8374.

References

Aagaard, P., Egeberg, P.K., Saigal, G.C., Morad, S., and Bjørlykke, K. (1990) Diagenetic albitization of detrital K-feldspars in Jurassic, Lower Cretaceous and Tertiary clastic reservoir rocks from offshore Norway, II. Formation water chemistry and kinetic considerations. *J. Sediment. Petrol.*, **60**, 575–81.

Aberdam, D. (1965) Utilisation de la microscopie electronique pour l'etude des feldspaths. Observations sur des microperthites. *Sci. de la Terre*, **6**, 76 pp.

Aldahad, A.A., and Morad, S. (1987) A SEM study of dissolution textures of detrital feldspars in Proterozoic sandstones, Sweden. *Amer. J. Sci.*, **287**, 460–514.

Atkinson, B.K. (1982) Subcritical crack propagation in rocks: theory, experimental results and applications. *J. Struct. Geol.*, **4**, 41–56.

Berner, R.A., and Holdren, G.R. (1977) Mechanism of feldspar weathering: Some observational evidence. *Geology*, **5**, 369–72.

Berner, R.A., and Holdren, G.R. (1979) Mechanism of feldspar weathering-II. Observations of feldspars from soils. *Geochim. Cosmochim. Acta*, **43**, 1173–86.

Bernotat-Wulf, H., Bertelmann, D. and Wondratschek, H. (1988) The annealing behaviour of Eifel sanidine

(Volkesfeld) III. The influence of the sample surface and the sample size on the order-disorder transformation rate. *N. Jb. Miner. Mh*, **11**, 503–15.

Bevan, J., and Savage, D. (1989) The effect of organic acids on the dissolution of K-feldspar under conditions relevant to burial diagenesis. *Mineral. Mag.*, **53**, 415–25.

Blum, A.E. (1994) Feldspars in weathering. In *Feldspars and their reactions.* (I. Parsons, ed.), NATO ASI Series, C421, Kluwer Academic Publishers, Dordrecht, 595–630.

Boldryev, V.V. (1979) Control of the reactivity of solids. *Ann. Rev. Mater. Sci.*, **9**, 455–69

Bradbury, M.H., and Green, A. (1986) Retardation of radionuclide transport by fracture flow in granite and argillaceous rocks. *Commission of the European Communities, Nuclear Science and Technology, Final Report EUR 10619 EN.*

Brown, W.L., and Willaime, C. (1974) An explanation of exsolution orientations and residual strain in cryptoperthites. In *The feldspars* (W.S. MacKenzie and J. Zussman, eds.), Manchester University Press, 440–59.

Brown, W.L. and Parsons, I. (1984) The nature of potassium feldspar, exsolution microtextures and development of dislocations as a function of composition in perthitic alkali feldspars. *Contrib. Mineral. Petrol.*, **86**, 335–341

Brown, W.L. and Parsons I (1988) Zoned ternary feldspars in the Klokken intrusion: exsolution textures and mechanisms. *Contrib. Mineral. Petrol.*, **98**, 444–454

Brown, W.L. and Parsons, I. (1989) Alkali feldspars: ordering rates, phase transformations and behaviour diagrams for igneous rocks. *Mineral. Mag.*, **54**, 25–42.

Brown, W.L. and Parsons, I. (1993) Storage and release of elastic strain energy: the driving force for low-temperature reactivity and alteration of alkali feldspar. In *Defects and processes in the solid state: geoscience applications. The Mclaren volume* (J. Boland and J.D. Fitz Gerald, eds.), Elsevier Science Publishers BV, Amsterdam, 267–90.

Brown, W.L. and Parsons, I. (1994) Feldspars in igneous rocks. In *Feldspars and their reactions* (I. Parsons, ed.), NATO ASI Series, C421, Kluwer Academic Publishers, Dordrecht, 449–99.

Brown, W.L., Becker, S.M., and Parsons, I. (1983) Cryptoperthites and cooling rate in a layered syenite pluton: a chemical and TEM study. *Contrib. Mineral. Petrol.*, **82**, 13–25.

Burgess, R. and Parsons, I. (1994) Argon and halogen geochemistry of hydrothermal fluids in the Loch Ainort granite, Isle of Skye, Scotland. *Contrib. Mineral. Petrol.*, **114**, 345–55.

Burgess, R., Kelley, S.P., Parsons, I., Walker, F.D.L. and Worden, R.H. (1992) ^{40}Ar–^{39}Ar analysis of perthite microtextures and fluid inclusions in alkali feldspars from the Klokken syenite, South Greenland. *Earth Planet. Sci. Lett.*, **109**, 147–67.

Chapman, N.A. and McKinley, I.G. (1987) *The Geological Disposal of Nuclear Waste.* John Wiley and Sons, Chichester, 280 pp.

Conover, W.J. (1980) *Practical non-parametric statistics.* 2nd Edn., Wiley. 493 pp.

Crampin, S. and Lovell, J.H. (1991) A decade of shear-wave splitting in the Earth's crust: what does it mean? what use can we make of it? and what should we do next? *Geophys. J. Int.*, **107**, 387–407.

Crampin, S. and Leary, P. (1993) Limits to crack density: the state of fractures in crustal rocks. *63rd Ann. Int. SEG Meeting, Washington, Expanded Abstracts*, 758–61.

Dengler, L. (1976) Microcracks in crystalline rocks. In *Electron microscopy in mineralogy* (H.R. Wenk, ed.), Springer, Berlin, Heidelberg, New York, 550–6.

Dodson, M.H. (1973) Closure temperature in cooling geochronological and petrological systems. *Contrib. Mineral. Petrol.*, **40**, 259–74.

Eggleton, R.A. and Buseck, P.R. (1980) High resolution electron microscopy of feldspar weathering. *Clays Clay Minerals*, **28**, 173–8.

Farver, J.R. and Yund, R.A. (1990) The effect of hydrogen, oxygen, and water fugacity on oxygen diffusion in alkali feldspar. *Geochim. Cosmochim. Acta*, **54**, 2953–64

Ferry, J.M. (1985) Hydrothermal alteration of Tertiary igneous rocks from the Isle of Skye, northwest Scotland. II. Granites. *Contrib. Mineral. Petrol.*, **91**, 283–304.

Fitz Gerald J.D and Harrison, T.M. (1993) Argon diffusion domains in K-feldspar 1: microstructures in MH-10. *Contrib. Mineral. Petrol.*, **113**, 367–80.

Folk, R.L. (1955) Note on the significance of 'turbid' feldspars. *Amer. Mineral.*, **40**, 356–7.

Foland, K.A. (1994) Argon diffusion in feldspars. In *Feldspars and their reactions* (I. Parsons, ed.), NATO ASI Series, C421, Kluwer Academic Publishers, Dordrecht, 415–47.

Foster, D.A., Harrison, T.M., Copeland, P. and Heizler, M.T. (1990) Effects of excess argon within large diffusion domains on K-feldspar age spectra. *Geochim. Cosmochim. Acta*, **54**, 1699–708.

Frost, B.R. and Bucher, K. (1994) Is water responsible for geophysical anomalies in the deep continental crust? A petrological perspective. *Tectonophysics*, **231**, 293–309.

Frost, B.R., Fyfe, W.S., Tazaki, K. and Chan, T. (1989) Grain-boundary graphite in rocks and implications for high electrical conductivity in the lower crust. *Nature*, **340**, 134–6

Fung, P.C., Bird, G.W., McIntyre, N.S., Sanipelli, G.G., Lopata, V.J. (1980) Aspects of feldspar dissolution.

Nuclear Technology, **51**: 188–96.

Gandais, M., Guillemin, C. and Willaime, C. (1974) Study of boundaries in cryptoperthites. *Eighth Int. Cong. Elec. Micros., Canberra*, 508–9

Giletti, B.J. (1985) The nature of oxygen transport within minerals in the presence of hydrothermal water and the role of diffusion. *Chem. Geol.*, **53**, 197–206.

Giletti, B.J. (1991) Rb and Sr diffusion in alkali feldspars, with implications for cooling histories of rocks. *Geochim. Cosmochim. Acta*, **55**, 1331–43.

Giletti, B.J. (1994) Isotopic equilibrium/disequilibrium and diffusion kinetics in feldspars. In *Feldspars and their reactions* (I. Parsons, ed.) NATO ASI Series, C421, Kluwer Academic Publishers, Dordrecht, 351–82.

Göttlicher, J. and Kroll, H. (1990) Order/disorder transformation in $KGaSi_3O_8$. Third International Symposium of Experimental Mineralogy, Petrology and Geochemistry, Edinburgh. *Terra Abstracts*, **2**, 77.

Graham, C.M. and Elphick, S.C. (1994) Hydrogen in feldspars and related silicates. In *Feldspars and their reactions* (I. Parsons, ed.), NATO ASI Series, C421, Kluwer Academic Publishers, Dordrecht, 383–414.

Grisak, G.E. and Pickens, J.F. (1980) Solute transport through fractured media, I: the effect of matrix diffusion. *Water. Resources Res.*, **16**, 719–30.

Guthrie, G.D. and Veblen, D.R. (1991) Turbid alkali feldspars from the Isle of Skye, northwest Scotland. *Contrib. Mineral. Petrol.*, **108**, 298–304.

Harrison, T.M. (1990) Some observations on the interpretation of feldspar $^{40}Ar/^{39}Ar$ results. *Chem. Geol. (Isotope Geoscience Section)*, **80**, 219–29.

Harrison, T.M., Heizler, M.T. and Lovera, O.M. (1993) *In vacuo* crushing experiments and K-feldspar thermochronometry. *Earth Planet. Sci. Lett.*, **117**, 169–80.

Harrison, T.N., Parsons, I. and Brown, P.E. (1990) Mineralogical evolution of fayalite-bearing rapakivi granites from the Prins Christians Sund pluton, South Greenland. *Mineral. Mag.*, **54**, 57–66.

Helgeson, H.C., Murphy, W.M. and Aagaard, P. (1984) Thermodynamic and kinetic constraints on reaction rates among minerals and aqueous solutions. II. Rate constants, effective surface area and the hydrolysis of feldspar. *Geochim. Cosmochim. Acta*, **48**, 2405–32.

Holdren, G.R. Jr. and Berner, R.A. (1979) Mechanism of feldspar weathering. – I. Experimental studies. *Geochim. Cosmochim. Acta*, **43**, 1161–71.

Holdren, G.R. Jr., Casey, W.H., Westrich, H.R., Carr, M. and Boslough, M. (1988) Bulk dislocation densities and dissolution rates in a calcic plagioclase. *Chem. Geol.*, **70**, 79.

Hyndman, R.D. and Shearer, P.M. (1989) Water in the lower continental crust: modelling magnetotelluric and seismic reflection results. *Geophys. J. Int.*, **98**, 343–65.

Hunter, R.F. (1987) Textural equilibrium in layered igneous rocks. In *Origins of Igneous Layering* (I. Parsons, ed.), NATO ASI Series, C196, D. Reidel, Dordrecht, 473–503.

Jones, A.G. (1992) Electrical conductivity of the continental lower crust. In *Continental Lower Crust* (D.M. Fountain, R.J. Arculus and R.W. Kay, eds.), Elsevier, 81–143.

Keller, W.D. (1978) Kaolinization of feldspar as displayed in scanning electron micrographs. *Geology*, **6**, 184–8.

Lasaga, A.C. and Blum A.E. (1986) Surface chemistry, etch-pits and mineral water reactions. *Geochim. Cosmochim. Acta*, **50**, 2363–79.

Leary, P.C. (1991) Deep borehole evidence for fractal distribution of fractures in crystalline rock. *Geophys. J. Int.*, **107**, 615–27.

Lee, M.R. and Parsons, I. (in press) Microtextural controls of weathering of perthitic alkali feldspars. *Geochimica Cosmochimica Acta.*

Lee, M.R., Waldron, K.A. and Parsons, I. (1995) Exsolution and alteration microtextures in alkali feldspar phenocrysts from the Shap granite. *Mineral. Mag.*, **59**, 63–78.

Lee, M.R., Waldron, K.A., Parsons, I. and Brown, W.L. (in prep) Mechanisms of fluid–feldspar interaction: pleated rims and the development of vein perthite. *Contrib. Mineral. Petrol.*

Lidiak, E.G. and Ceci, V.M. (1991) Authigenic K-feldspar in the Precambrian basement of Ohio and its effect on tectonic discrimination of the granitic rocks. *Can. J. Earth Sci.*, **28**, 1624–34.

Lloyd, G.E. and Knipe, R.J. (1992) Deformation mechanisms accomodating faulting of quartzite under upper crustal conditions. *J. Struct. Geol.*, **14**, 127–43

Lovera, O.M., Richter, F.M. and Harrison, T.M. (1989) The $^{40}Ar/^{39}Ar$ thermochronometry for slowly cooled samples having a distribution of diffusion domain sizes. *J. Geophys. Res.*, **94, B12,** 17917–35

Lovera, O.M., Richter, F.M. and Harrison, T.M. (1990) Diffusion domains determined by ^{39}Ar released during step heating. *J. Geophys. Res.*, **96, B2**, 2057–69

Lundström, I. (1974) Etch pattern and albite twinning in two plagioclases. *Arkiv. Mineral. Geologi.*, **5**, 63–91.

Manning, D.A.C., Rae, E.I.C. and Small, J.S. (1991) An exploratory study of acetate decomposition and dissolution of quartz and Pb-rich potassium feldspar at 150°C, 50 MPa (500 bars). *Mineral. Mag.*, **55**, 183–95.

Mareschal, M., Fyfe, W.S., Percival, J. and Chan, T. (1992) Grain-boundary graphite in Kapuskasing gneisses and implications for lower crustal

conductivity. *Nature*, **357**, 674–6.

McDowell, S.D. (1986) Compositional and structural state of coexisting feldspars, Salton Sea geothermal field. *Mineral. Mag.*, **50**, 75–84.

Meike, A. (1990) A micromechanical perspective on the role of dislocations in selective dissolution. *Geochim. Cosmochim. Acta*, **54**, 3347–52.

Montgomery, C.W. and Brace, W.F. (1975) Micropores in plagioclase. *Contrib. Mineral. Petrol.*, **52**, 17–28.

Murphy, W.M. (1989) Dislocations and feldspar dissolution. *Euro. J. Min.*, **1**, 315–26.

Neretnieks, I. (1980) Diffusion in a rock matrix: an important factor in radionuclide retardation? *J. Geophys. Res.*, **85**, 4379–97.

Nesbitt, H.W., MacRae, N.D. and Shotyk, W. (1991) Congruent and incongruent dissolution of labradorite in dilute, acidic, salt solutions. *J. Geol.*, **99**, 429–42.

Neumann, D. and Rutter, E.H. (1994) Experimental deformation of partially molten Westerly granite under vapour-absent conditions. *Terra Abstracts, supplement No. 1 to Terra Nova*, **6**, 35.

Nixon, R.A. (1979) Differences in incongruent weathering of plagioclase and microcline–cation leaching versus precipitates. *Geology*, **7**, 221–4.

O'Neill, J.R. and Taylor, H.P. (1967) The oxygen isotope and cation exchange chemistry of feldspars. *Amer. Mineral.*, **52**, 1414–37.

Parsons, I. (1978) Feldspars and fluids in cooling plutons. *Mineral. Mag.*, **42**, 1–17.

Parsons, I. (1980) Alkali-feldspar and Fe-Ti oxide exsolution textures as indicators of the distribution and subsolidus effects of magmatic 'water' in the Klokken layered syenite intrusion, South Greenland. *Trans. Roy. Soc. Edinburgh.: Earth Sci.*, **71**, 1–12.

Parsons, I. and Brown, W.L. (1984) Feldspars and the thermal history of igneous rocks. In *Feldspars and feldspathoids: structure and occurrence.* (W.L. Brown, ed.), NATO ASI Series, Reidel, Dordrecht, 317–71.

Parsons, I., Rex, D.C., Guise, P. and Halliday, A.N. (1988) Argon-loss by alkali feldspars. *Geochim. Cosmochim. Acta*, **52**, 1097–112.

Parsons, I., Mason, R.A., Becker, S.M. and Finch, A.A. (1991) Biotite equilibria and fluid circulation in the Klokken Intrusion. *J. Petrol.*, **32**, 1299–333.

Poldervaart, A. and Gilkey, A.K. (1954) On clouded plagioclase. *Amer. Mineral.*, **39**,: 75–91

Richter, F.M., Lovera, O.M., Harrison, T.M. and Copeland, P. (1991) Tibetan tectonics from $^{40}Ar/^{39}Ar$ analysis of a single K-feldspar sample. *Earth Plan. Sci. Lett.*, **105**, 266–78

Rickert, P.G., Strickert, R.G. and Seitz, M.G. (1979) Nuclide migration in fractured or porous rock. In *Radioactive Waste in Geologic Storage* (S. Fried, ed.), American Chem Soc, Washington, 167–90.

Roedder, E. (1984) *Fluid Inclusions*. Mineral. Soc. Amer. Reviews in Mineralogy, **12**, 646.

Roedder, E. and Coombs, D.S. (1967) Immiscibility in granitic melts, indicated by fluid inclusions in ejected granite blocks from Ascension Island. *J. Petrol.*, **8**, 417–51.

Saigal, G.C., Morad, S., Bjørlykke, K., Egeberg, P.K. and Aagaard, P. (1988) Diagenetic albitization of detrital K-feldspar in Jurassic, Lower Cretaceous and Tertiary clastic reservoir rocks from offshore Norway, I: Textures and origin. *J. Sediment. Petrol.*, **58**, 1003–13.

Seifert, K.E. (1967) Electron microscopy of etched plagioclase feldspar. *Journ. Amer. Ceram. Soc.* **50**, 660–1

Smith, J.V. and Brown, W.L. (1988) *Feldspar Minerals 1. Crystal Structures, Physical, Chemical and Microtextural Properties*. Springer-Verlag, Berlin, Heidelberg, New York, 828 pp.

Sprunt, E.S. and Brace, W.F. (1974) Direct observations of microcavities in crystalline rocks. *Int. J. Rock Mech. Min. Sci. & Geomech. Abstr.*, **11**, 139–50.

Taylor, H.P. and Forester, R.W. (1971) Low-O^{18} igneous rocks from the intrusive complexes of Skye, Mull, and Ardnarmurchan, Western Scotland. *J. Petrol.*, **12**, 465–98

Tazaki, K. and Fyfe, W.S. (1987) Primitive clay precursors formed on feldspars. *Can. J. Earth Sci.*, **24**, 506–27.

Tchoubar, C. (1965) Formation de la kaolinite à partir d'albite altérée par l'eau à 200°C. Etude en microscopie et diffraction électroniques. *Bull. Soc. Franç. Min. Crist.*, **88**, 483–518.

Tullis, J. (1975) Elastic strain effects in coherent perthitic feldspars. *Contrib. Mineral. Petrol.*, **49**, 83–91.

Tullis, J. and Yund, R.A. (1977) Experimental deformation of dry Westerly granite. *J. Geophys. Res.*, 82, 5705–17.

Tullis, J. and Yund, R.A. (1979) Calculation of coherent solvi for alkali feldspar, iron-free clinopyroxene, nepheline–kalsilite, and hematite–ilmenite. *Amer. Min.*, **64**, 1063–74

Tuttle, O.F. (1952) Origin of the contrasting mineralogy of extrusive and plutonic salic rocks. *J. Geol.*, **60**, 107–24.

Velbel, M.A. (1986) Influence of surface area, surface characteristics and solution composition on feldspar weathering rates. In *Geochemical processes at mineral surfaces* (J.A. Davis and K.F. Hayes, eds.), Amer. Chem. Soc, 615–34.

Villa, I.M. (1994) Multipath Ar transport in K-feldspar deduced from isothermal heating experiments. *Earth Planet. Sci. Lett.*, **122**, 393–401.

Waldron, K.A. and Parsons, I. (1992) Feldspar microtextures and multistage thermal history of syenites from the Coldwell Complex, Ontario. *Contrib. Mineral. Petrol.*, **111**, 222–34.

Waldron, K.A., Parsons, I. and Brown, W.L. (1993)

Solution-redeposition and the orthoclase–microcline transformation: evidence from granulites and relevance to ^{18}O exchange. *Mineral. Mag.*, **57**, 687–95.

Waldron, K.A., Lee, M.R. and Parsons, I. (1994) The microstructures of perthitic alkali feldspars revealed by hydrofluoric acid etching. *Contrib. Mineral. Petrol.*, **116**, 360–64.

Walker, F.D.L. (1990) Ion microprobe study of intragrain micropermeability in alkali feldspars. *Contrib. Mineral. Petrol.*, **106**, 124–8.

Walker, F.D.L. (1991) *Micropores in Alkali Feldspars.* Unpublished PhD thesis, University of Edinburgh.

White, J.C. and Barnett, R.L. (1990) Microstructural signatures and glide twins in microcline, Hemlo, Ontario. *Can. Mineral.*, **28**, 757–69.

Wilson, M.J. (1975) Chemical weathering of some primary rock-forming minerals. *Soil Sci.*, **119**, 349–55.

Wilson, M.J. and McHardy, W.J. (1980) Experimental etching of a microcline perthite and implications regarding natural weathering. *J. Microscopy*, **120**, 291–302.

Worden, R.H. and Rushton, J.C. (1992) Diagenetic K-feldspar textures: a TEM study and model for K-feldspar growth. *J. Sediment. Petrol.*, **62**, 779–89.

Worden, R.H., Walker, F.D.L., Parsons, I. and Brown, W.L. (1990) Development of microporosity, diffusion channels and deuteric coarsening in perthitic alkali feldspars. *Contrib. Mineral. Petrol.*, **104**, 507–15.

[*Manuscript received 5 December 1994: revised 3 January 1995*]